Brushless Doubly-Fed Machines: Opportunities and Challenges

Peng Han[1], *Ming Cheng*[1]*, *Sul Ademi*[2], *and Milutin G. Jovanović*[3]

(1. School of Electrical Engineering, Southeast University, Nanjing 210096, China;
2. Warwick Manufacturing Group, University of Warwick, Coventry, UK;
3. Faculty of Engineering and Environment, Northumbria University, Newcastle upon Tyne, UK)

Abstract: The brushless doubly-fed machine(BDFM) is a family of multiport electric machines with two ac electrical ports and a common mechanical port. Different from the conventional singly-fed machines whose synchronous speed is solely determined by a single supply frequency and the actual pole pair number, the BDFM has two supply frequencies and two different pole pair numbers to control the rotor speed. By the two accessible electrical ports, all BDFMs are endowed with more degrees of freedom for speed and power control, inherent fault-tolerant capability and high reliability. The BDFM in its broad sense has been extensively investigated as a promising alternative to the conventional slip-ring doubly-fed induction machine(DFIM) during the past decades, for both limited and wide speed range applications. This paper presents a new theoretical framework of the BDFM within which all topological variants can be closely linked by the similarities in working principle. The individualities of each machine topology are presented first, followed by the commonalities such as the modeling techniques, modes of operation, design considerations and control strategies. The challenges are identified and highlighted based on recent developments and possible opportunities are predicted considering the unique nature of this special AC machine type.

Keywords: Brushless doubly-fed machine, multiport electric machine, modeling techniques, modes of operation, design considerations, control strategies.

1 Introduction

Doubly-fed machines(DFMs), including the traditional slip-ring doubly-fed induction machine(DFIM) and various brushless versions, pertain to the emerging multiport electrical machines and play an indispensable role in efficient and flexible energy conversion, transfer and/or recovery. Recent research trends in this broad area have highlighted the distinct advantages of brushless doubly-fed machines(BDFMs) over the slip-ring DFIM and even conventional singly-fed machines in some aspects, such as the enhanced reliability due to the robust brushless rotor configuration and multiple modes of operation, the low-cost fractionally-rated power electronics converter for limited speed range applications, flexible control of active and reactive power, crowbarless low voltage ride-through(LVRT) grid integration capability, etc., showing their promising prospects in variable speed drive and generation systems. It is worth noting that by the BDFM term the authors do not refer to the specific construction with a nested-loop or reluctance rotor, but rather to a family of brushless AC machines of the following common features:

- There are two relatively independent AC electrical ports [i.e., power winding(PW) and control winding (CW)] with the ability to handle bidirectional power flow on the stator.
- There is a single physical mechanical port(the shaft) to input or output mechanical power.
- Doubly-fed synchronous operation can be realized.
- Asynchronous operation is possible if one of the two electrical ports is short-circuited.

* Corresponding Author, Email: mcheng@seu.edu.cn.

A broad body of work has been published during the past years and this paper aims at providing an up-to-date reference of the published work and the systematic background knowledge by developing a new theoretical framework of the BDFM in its broad sense to help research and industrial communities keep track of the recent progress in this fast-growing area.

To the best of the authors' knowledge, the first attempt to categorize the DFMs was made in 2001[1]. The frequency behavior, power flow, modeling and control aspects of the DFIM and its brushless counterparts were mainly focused on, and a brief comparison in terms of ease of manufacture, converter rating and control complexity was conducted in this work to foresee the commercial future of different topologies. A historical evolution of cascading two DFIMs into the modern brushless DFIM (BDFIM) is detailed in [2]. The control methods for the brushless doubly-fed reluctance machine (BDFRM) have been reviewed in [3]. Starting with a concise description of the origin and development of BDFMs with nested-loop and reluctance rotors, the material presented in [4] places more emphasis on the structural diversity of rotor topologies.

This paper is concerned with the available designs, operating modes and applications of the BDFM in a totally different manner from, and in many respects it augments in content, the reviews hitherto published on the subject[1-4]. The work is also closely relevant to research on brushless electrically-excited synchronous machines(EESMs) and multiphase machines. It is organized as follows. Section 2 deals with the proposed classification and key definitions related to BDFMs. Section 3 overviews the basic topologies, working principles and electromagnetic performances of a wide

variety of BDFMs reported in the literature. Section 4 describes the modeling issues, whereas the modes of operation and the main target applications are summarized in Section 5. In Sections 6 and 7, the considerations in design of BDFMs(torque ripples and time-harmonic distortion, iron saturation effects, core losses, vibration and acoustic noise) and control strategies, mainly including the mostly studied field oriented control(FOC) and direct control methods, are presented. Concluding remarks and directions for further research are given in Section 8.

2 Classification and key definitions

All BDFMs can be conceptually conceived as the outgrowths of removing the brush gear of the DFIM, which can be generally accomplished either by PM excitation, cascading or modulation. The PM excitation reduces the number of ac electrical ports and as such is excluded from the scope of BDFMs. Cascading means maintaining the basic DFIM configuration with an extra power device to transfer power onto the rotor winding in a contactless fashion, while the modulation represents a sophisticated utilization of short-circuited coils, variable reluctance or flux guides to provide magnetic cross-coupling between two distributed stator windings of different pole pairs[5]. Either way, the stator windings—PW and CW, are indirectly coupled through the rotor action, as illustrated in Fig.1.

With respect to the cascading type, the contactless power transfer from a static power supply to the rotor winding can be achieved by cascading another DFIM (within the same frame or not) or using a rotary transformer (RT). Consequently, the cascaded DFIM (CDFIM)[6] and the DFIM with RT(DFIM-RT)[7] come to realization.

As for the modulation type, the rotor structure is of utmost importance because it provides the only means to indirectly couple the stator windings through the airgap field modulation behavior. To this extent, the rotor can be designed with short-circuited coils, salient-pole blocks or flux-barrier segments. The short-circuited coils give birth to the nested-loop rotor BDFIM and multi-layer wound rotor BDFIM[8], while the salient-pole blocks and flux-barrier segments bring about the BDFRM[9], whose rotor usually takes three different forms in practice, namely, the simple salient pole, the multi-layer flux-barrier, and the axially laminated design. A number of hybrid rotors can be further derived from these basic rotor constructions. For instance, the hybrid rotor in [10] is virtually a combination of short-circuited coils and flux-barrier segments. The magnetic circuit optimization is realized by introducing flux-barrier blocks into the BDFIM with a nested-loop rotor[11]. A detailed classification of the BDFM is shown in Fig.2.

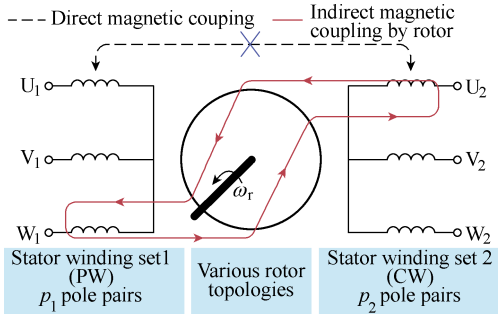

Fig.1 The schematic diagram of the BDFM in its broad sense

Thanks to this classification based on operating principles, previous research on all BDFMs can be reorganized in a unified way. Though differing a lot in terms of structure(i.e., the structural diversity), BDFM topologies of the same type considered in Section 1 share nearly the same vector models, modes of operation, design aspects and control strategies, as will be discussed in detail in Sections 3~7. The key definitions and angular velocity relationships are introduced here first in order to characterize the operation of all BDFMs in consistent terminologies though some of them have already been proposed for the BDFIM with a nested-loop rotor[12].

There are in total three synchronous speeds in BDFMs, i.e., the PW-synchronous speed(ω_p/p_p), the CW-synchronous speed(ω_c/p_c) and the doubly-fed synchronous speed (ω_s), which can be expressed as:

$$\omega_s=\frac{\omega_p \pm \omega_c}{p_{eq}} \tag{1}$$

where ω_p and ω_c are angular frequencies of the $2p_p$-pole PW and $2p_c$-pole CW, respectively, and p_{eq} denotes the number of equivalent pole pairs. The latter can either be the sum or the absolute difference of p_p and p_c. The cascading (or modulation) type is termed as sum cascading (or sum modulation) only if $p_{eq}=p_p+p_c$, where the torques produced by the p_p and p_c pole pair magnetic fields are co-acting. On the contrary, the cascading (or modulation) type is termed as difference cascading (or difference modulation) if $p_{eq}=|p_p-p_c|$, where these torques are counter-acting. Therefore, the sum cascading (modulation) is usually used for high torque and low speed applications whereas the difference cascading (modulation) is more suitable for high speed operation[8]. In the modulation version (sum or difference modulation), p_p and p_c should be different to avoid direct magnetic interaction between the stator windings. However, for the cascading type, $p_p \neq p_c$ is only required for the difference cascading, otherwise the machine turns out to be a tandem induction machine (IM) and (1) is no longer applicable. The BDFM works in doubly-fed synchronous mode, i.e., synchronous operation, only if the rotor speed is given by (1), otherwise, it is in asynchronous operation.

In a special case when the CW is fed by DC, the BDFM degrades into a brushless EESM, whose dc field winding and AC armature windings are located on the same stator core and indirectly coupled by a passive

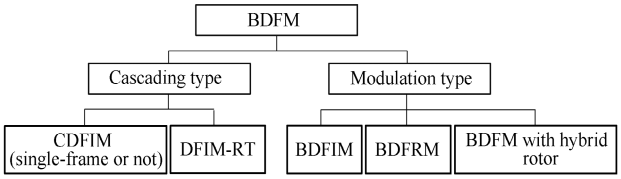

Fig.2 The classification of BDFMs

rotor, and the corresponding doubly-fed synchronous speed is then termed as natural synchronous speed, which is:

$$\omega_{\mathrm{n}}=\frac{\omega_{\mathrm{p}}}{p_{\mathrm{eq}}} \tag{2}$$

The BDFM works in natural synchronous operation only if it runs at the natural synchronous speed formulated by (2). Below this speed, it is operated in the sub-natural-synchronous mode, and if above, it enters the super-natural-synchronous mode. Similarly, the BDFM is in super-PW-synchronous mode if the rotor speed exceeds the PW-synchronous speed. The synchronous speeds and associated operating modes are summarized in Fig.3 for convenience.

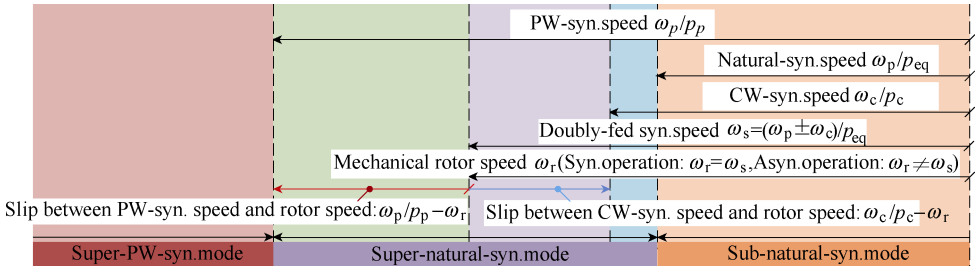

Fig.3 Synchronous speeds and operating modes of BDFMs

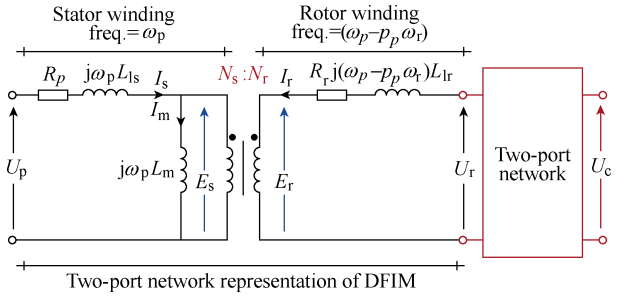

Fig.4 Operating principle of the cascading type from the point of view of electric circuit theory

Once DC components, such as DC excitation windings or uncontrollable rectifiers appear in the cascade system, the whole system will become singly-fed because one of the two electrical ports loses the capability for bidirectional power flow. Typical examples are the classical multi-stage synchronous generator with brushless excitation and the recently proposed synchronous machine(SM) with capacitive power transfer[13]. The brushless system realized by cascading a DFIM with an inverted SM via a rotating power converter also turns out to be a singly-fed one, though it is also sometimes termed as BDFIM in the literature [14].

3.1.1 CDFIM

The CDFIM is the ancestor of BDFMs and can be dated back to the cascade concept in poly-phase traction motors[6]. A typical cascading system comprised of two DFIMs is schematically depicted in Fig.5(a), whereby the two IMs are arranged with the shaft mechanically coupled and slip-rings of the primary motor connected to the stator windings of the secondary motor. The stator

3 Basic topologies and fundamental principles

3.1 Cascading type

This BDFM type can be explained straightforwardly by the electrical equivalent circuit (EEC). As illustrated in Fig.4, the DFIM has directly-coupled stator and rotor windings and is therefore equivalent to a two-port network. The two-port structure will remain by connecting an additional two-port network to the DFIM in cascade, while eliminating the brushes and slip rings in the process. The two-port network can be another DFIM or a transformer. It is obvious that there is no direct coupling between the two stator windings of the cascading type due to the spatial separation.

windings of the primary motor are directly fed from the main supply, while the slip-rings of the secondary motor are short-circuited through the starting or regulating resistances, i.e., the rheostats. To avoid the unreliable slip-rings, the cascade connection between the two rotors (instead of rotor-stator) was proposed, resulting in the well-recognized configuration of CDFIM shown in Fig.5(b)[15]. Note that, to achieve the sum cascading, the stator and rotor windings in Fig.5(a) should be connected in the same phase sequence (i.e., a-A, b-B, c-C), but for the CDFIM in Fig.5(b), the two rotor windings should be connected with the reversed phase sequence (i.e., a-c, b-b, c-a). The synchronous torque characteristic produced in doubly-fed operating mode is quite similar to the conventional SM, as will be shown in Section 5. However, apart from the desired synchronous torque, there are some non-zero parasitic asynchronous torque components caused by the rotor

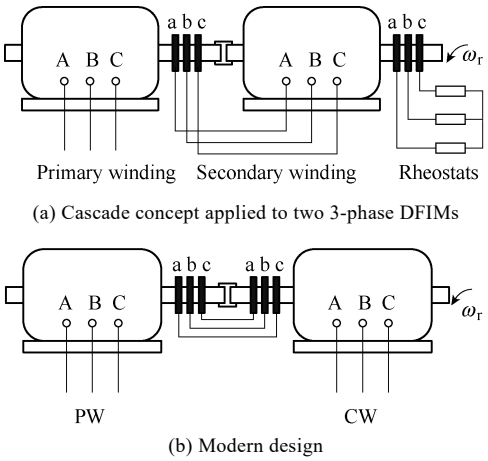

Fig.5 The CDFIM evolution

resistance (corresponding to the d-q axes cross-coupling phenomena) that increase the control complexity especially near the PW-synchronous speed. The pole-pair combination has been recommended to meet the $p_p \geqslant p_c$ constraint for better performance in terms of power flow, converter size, system efficiency and machine utilization[16].

Though it is theoretically feasible to cascade any two DFIMs to form a CDFIM, it is still unclear as to what kind of combination will be the optimal for the cascading construction. Sometimes, the two stators are enclosed in the same frame and the interconnected rotors are replaced by a crossover squirrel-cage rotor to form the single-frame CDFIM. To reduce the envelope volume and improve the mechanical integrity of the CDFIM, an intuitive idea of integrating a small IM into the internal vacancy of the DFIM brings about the dual-stator BDFIM(DS-BDFIM) design[17]. A non-magnetic rotor support layer is always required to eliminate the direct coupling between the two magnetic fields traveling in the inner and outer airgaps.

3.1.2 DFIM-RT

The DFIM-RT is a DFIM cascaded by a RT, which enables contactless inductive power transfer to the rotor winding from a static power converter, as illustrated in Fig.6[7]. It can be regarded as a special case of the CDFIM when the number of pole pair of CW is set to null. In contrast to the CDFIM, the control side produces no parasitic asynchronous torque due to the permanent alignment of the rotor and the stator windings of the RT. Generally, the option of using three single-phase transformers is preferable to avoid unbalanced magnetizing flux. Both radial and axial airgaps can be adopted, except that the latter introduces axial force on the bearing due to magnetic attraction.

3.2 Modulation type

Unlike the cascaded version, the BDFM modulation type relies on the asynchronous modulation behavior of the specially-designed rotors. The operating principles can be explained by the general airgap field modulation theory[5]. The primitive magnetizing magnetomotive force (MMF) established by one of the stator windings, is asynchronously modulated by the rotor to generate a full spectrum of MMF harmonics, among which one principal harmonic couples the complementary stator winding to produce effective flux and electromotive force in generating mode or electro-magnetic torque by injecting current in motoring mode. Despite the apparent differences in rotor constructions, the modulated MMFs have a similar spectrum distribution, and the effective harmonic of $N_r - p_c$ (for the sum cascading or modulation) or $N_r + p_c$ (for the difference cascading or modulation) pole pairs takes a relatively large proportion in coupling with the complementary stator winding, where N_r is the number of rotor nests, rotor salient poles or multi-barrier segments. Since the PW and CW are accommodated in the same stator core, special care should be taken in the design process to avoid potential direct coupling between them, which is closely related to the pole pair combination, number of parallel paths, the winding type and winding connection[18-19].

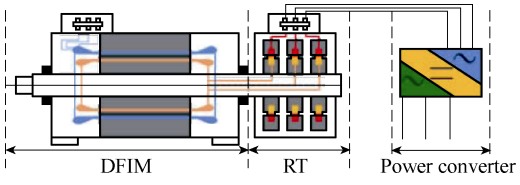

Fig.6 The DFIM-RT[7]

3.2.1 BDFIM

Research on pole changing and pole amplitude modulation winding created the idea of superseding the redundant rotor windings of self-cascading two DFIMs within a single magnetic circuit with a simple and robust nested-loop winding or multiphase double-layer winding[8]. To date, a number of rotor winding structures have been proposed, such as the nested-loop winding with a common ring, isolated nested-loop winding, nested-loop winding with two common rings[20], series-loop winding[21] and multi-phase double-layer winding with equal or unequal turn coils[22], as shown in Fig.7. Although all of them can perform the aforementioned field modulation and achieve cross-coupling between the PW and CW, they exhibit distinct differences in rotor resistance and leakage inductance levels, which significantly impact the electromagnetic performance (the degree of cross-coupling between PW and CW, torque density, efficiency, LVRT capability, etc.) and control properties as elaborated in [23-25]. Notice that the well-known nested-loop rotor which was originally invented for ease of manufacture, turns out to suffer from unequal rotor current distribution—the outer loop carries larger current and withstands higher temperature, leading to a high inter-bar current if uninsulated bars like die-cast squirrel-cage rotor for the IM is adopted[26]. In this respect, the series-loop winding and the multiphase double-layer winding with equal or unequal turn coils may outweigh the nested-loop one by equalizing the current distribution in conductors, with additional benefits of less severe MMF harmonic distortion and local iron saturation and lower hot spot temperature[21].

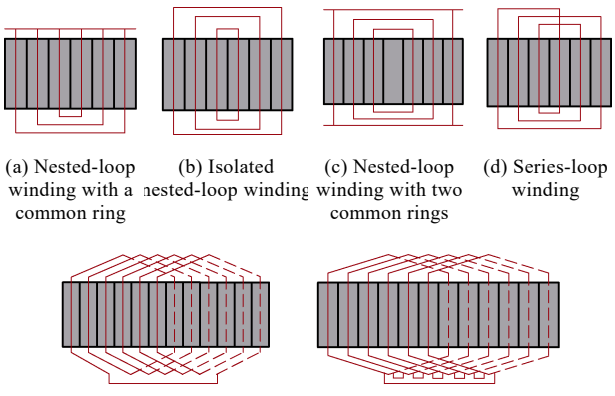

Fig.7 Available rotor winding structures for BDFIM

3.2.2 BDFRM

The idea that short-circuited coils of the BDFIM can be replaced by high-reluctance flux barriers to cause similar opposition to the magnetic flux has come through in the BDFRM[9]. It has been shown that any available rotor type used for synchronous reluctance machines (SynRMs) is essentially applicable in the BDFRM, i.e., the simple salient-pole rotor[27], axially-laminated anisotropic rotor[28] and multi-layer flux-barrier rotor[29] shown in Fig.8. The simple salient-pole rotor employs alternative variation of magnetic reluctance of salient-pole blocks to modify the harmonic spectrum of MMF distribution, while the axially-laminated anisotropic rotor and multi-layer flux-barrier rotor make full use of the non-uniform distribution of MMF along the airgap circumference to produce new spatial harmonic spectrums[5]. Whilst all of them can serve the purpose as the intermediate between the PW and CW, the performance like cross-coupling capability, torque density, core losses, etc., varies significantly with the rotor type, as discussed in [30-32]. An axial-flux dual-stator counterpart has been recently proposed to improve the torque density and enable the more flexible rotor pole shape design[33].

3.2.3 BDFM with a hybrid rotor

To further improve the cross-coupling capability, a hybrid rotor shown in Fig.9(a) which integrates short-circuited coils and multi-layer flux-barriers has been proposed, analyzed and used in a BDFM[34] and brushless EESM[10], the latter being a special case of the BDFM with dc supplied CW. A similar hybrid structure in Fig.9(b) has also been derived from the BDFIM with a nested-loop rotor by introducing axial ducts with an incentive to reduce the overall weight of the rotor. The ducts also serve as the flux barriers in isolating the magnetic circuits occupied by adjacent copper nests[11]. As a result, the rotor shown in Fig.9(b) can be treated as a combination of the nested-loop rotor and a flux-barrier rotor.

(a) Simple salient-pole (b) Axially-laminated anisotropic (c) Multi-layer flux-barrier

Fig.8 The BDFRM rotor designs (arrow: lamination direction)

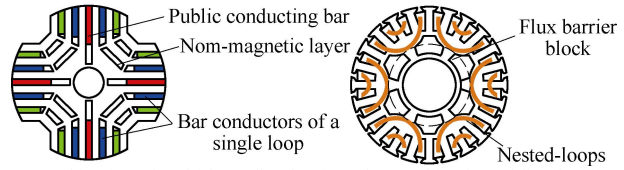

(a) Combination of multi-layer flux-barrier with short-circuited coils[10] (b) Combination of flux-barrier block with short-circuited coils[11]

Fig.9 Hybrid rotor configurations for the BDFM

4 Modeling techniques

Modeling approaches widely used for conventional ac machines, including the electromagnetic-field-based and electric-circuit-based, can be equally applied to the BDFMs. A detailed classification is shown in Fig.10.

4.1 Electromagnetic-field-based modeling

The one-dimensional harmonic analysis, assuming a linear magnetic circuit, is primarily used to explain the operating principles of the modulation type and to predict the frequency-domain characteristics for torque ripples, currents and voltages[20,35,36]. To accurately calculate the steady-state and dynamic performance of the BDFMs, especially with additional rotor circuit, iron losses and saturation effects considered, time-consuming time-stepping finite element analyses (FEAs) are usually conducted[37-39]. Various magnetic equivalent circuit (MEC) models[40-42] and a magnetostatic finite element (FE) method based on space-time transformations[43] were later developed to reduce the calculation time, while still maintaining acceptable results for the population-based optimization.

4.2 Electric-circuit-based modeling

The steady-state operation of the BDFM is normally studied using a per-phase EEC. The operating limits, maximum torque capability and volt-ampere requirements for control of the CDFIM were investigated by applying the standard EEC shown in Fig.11(a), albeit with parameters referred to the rotor side[44]. Two additional constant shunt core loss resistances were employed to improve the EEC quality in [16], with emphasis being made on frequency constraints for synchronous operation, active-reactive power flow, and converter rating. In order to account for the influence of core losses more accurately and to make the entire model realistic, variable iron loss resistances were added to both stator and rotor sides[45].

The standard EEC was also conceptually developed for the steady-state analysis of the BDFIMs by analogy to the conventional one for IMs[46] as depicted in Fig.11(a).

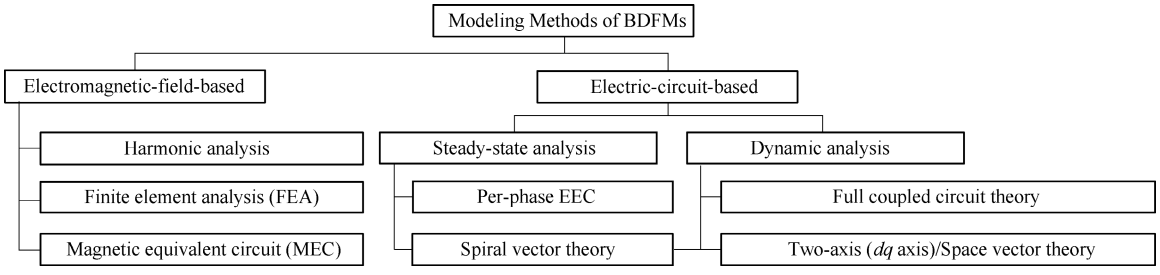

Fig.10 The classification of the BDFMs modeling methods

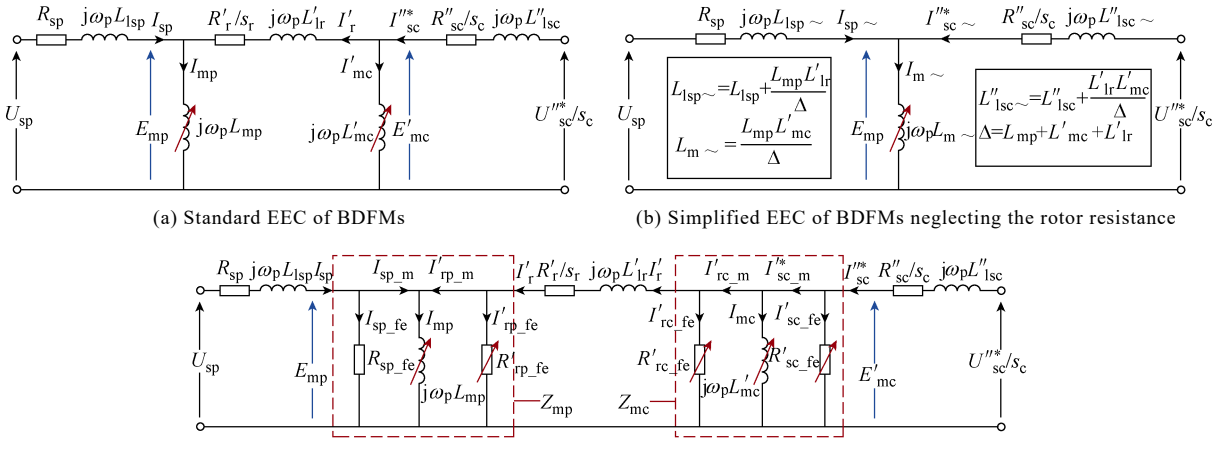

(a) Standard EEC of BDFMs

(b) Simplified EEC of BDFMs neglecting the rotor resistance

(c) EEC of BDFMs taking into account speed-dependent core losses and iron saturation

Fig.11 EECs of BDFMs with rotor windings and parameters referred to the PW side (note: resistances/inductances crossed by red arrows are variable)

The logic behind this was based on the perception that the BDFIMs can be functionally treated as two cascaded IMs built in the same frame. Considering that the BDFIM usually has a small rotor resistance and operates at relatively large slip frequency, the EEC can be simplified to that in Fig.11(b)[47]. The standard EEC can be further improved by integrating speed-dependent resistances in parallel with the PW and CW magnetizing branches to properly take core losses into consideration[48] as illustrated in Fig.11(c). Voltage equations in phasor notation and the corresponding steady-state EEC have also been derived to study the asynchronous and doubly-fed synchronous operation of BDFRM[9].

In the electric-circuit-based modeling, accurate parameter identification is challenging, especially for topologies with short-circuited rotor windings which is impossible to have a direct physical access without extra hardware. All the EEC parameters in the standard EEC depicted in Fig.11(a) (i.e., 3 resistances, 3 leakage inductances and 2 magnetizing inductances) can be readily calculated using the established empirical formulas and facilitated magnetic circuit methods for conventional machines[49-50], but the accuracy cannot be guaranteed since the BDFMs are usually designed with some degree of saturation to fully utilize the core material. Therefore, experimental extraction of parameters is more attractive. Standard no-load and locked-rotor tests for IMs were used in [51] with 1%~7% of the stator winding inductance being assigned to the leakage component for ease of parameter separation. An off-line estimation method in frequency domain was first implemented to find the resistances and inductances of the BDFIM for a range of excitation frequencies[52]. An alternative way is transforming the standard EEC to reduce the number of unknown parameters first and then curve-fitting the torque-speed characteristics obtained from both simple and cascade induction modes to complete the parameter estimation[46]. An off-line identification method using pseudo-random binary signal excitation and recursive least squares estimation was successfully applied to the BDFIM recently to determine the full EEC parameter set[53]. Given that the three resistances are measurable, the five inductances can be solved out by the semi-definite programming based on no-load and stand-alone load tests[54].

Even for the BDFRM which has no rotor windings, the high leakage inductances also adversely impact the accuracy of conventional off-line parameter testing, and open-circuit or pulse tests are recommended instead[55]. The practical BDFM dynamic models primarily include the full-coupled circuit model and the two-axis (*d-q*) or space-vector models in various reference frames. In the CDFIM case, the latter can be in power/control stator frame, rotating frames locked with the rotor or PW/CW flux (field), or even in an arbitrary reference frame as developed in [56]. The two- axis model for the BDFIM in a rotor frame was for the first time established for computer simulations[57], based upon which a rotor-FOC (RFOC) scheme with an unusual decoupling technique was proposed in [58]. However, the aforementioned models for the BDFIM with a nested-loop rotor have neglected the individual effects of multiple loops per nest by conceptually and unwarrantedly replacing them with an equivalent single loop. Such an approximation is essentially a model order reduction problem and it appears to be justified with a minimum loss of accuracy as initially observed in [59] and later solved in [60]. The reduced-order d-q model of the BDFIM in a unified reference frame was developed for the stator-flux-oriented controller design[61-62]. The most compact version of a space vector model with multi-loop circuit equations was subsequently built for BDFIM performance predictions and control without compromising much on accuracy[63]. Similarly, the fundamental theory and dynamic models of the BDFRM have also been developed and thoroughly investigated[64-66].

In addition to the ordinary modeling routines, several new methods have also been proposed, such as the dynamic EEC for CDFIM control by applying the inverse model principle[67], and the spiral vector modeling of the DS-BDFIM for unified steady-state and dynamic analysis[68].

5 Modes of operation

The presence of two physical electrical ports benefits the BDFMs with a variety of available operating modes,

which have been clearly defined and experimentally identified in [38, 68] and [69]. Note that in this section, the BDFM in all available modes of operation are not necessarily grid-connected. They can be supplied by converters too.

5.1 Simple induction mode

The BDFM works in this mode if one of the two electrical ports is open-circuited while the other is supplied. It only appears in BDFM topologies with rotor windings and is essentially an IM with a substantially increased secondary leakage inductance contributed by the magnetizing inductance of the open-circuited side. The torque capability is thus significantly reduced even when the rated voltage is applied, as depicted by the dash line in Fig.12(a). This mode of operation can be effectively used to measure the cross-coupling characteristics[45].

5.2 Cascade induction mode

If one of the two electrical ports is short-circuited and the other supplied, the BDFM will operate in the cascade induction mode. Taking the sum cascading (or sum modulation) case as an example, in the vicinity of the natural synchronous speed, the retarding torque coming from the interaction between the shorted stator windings and the rotor successfully prevents the rotor from exceeding the natural speed in motoring operation, so the BDFM can be fully controlled by external resistances connected to the CW or constant V/f supply connected to the PW as a motor. As indicated by the torque-speed characteristic (solid line in Fig.12(a)), the torque-curve in the full speed range is essentially the sum of two IMs, one with the pole pair number of the PW and the other the equivalent pole pair number (p_p+p_c). The torque production in this mode is comparable to that of a single IM within the cascade construction, so it can be used in practical motoring or generating regimes. A special application of the cascade induction mode is to start up the machine from standstill[70-72].

5.3 Singly-fed synchronous mode

If the two electrical ports are dc and ac fed, the BDFM rotor would be naturally locked into synchronism emulating a brushless EESM with (p_p+p_c) pole-pairs[10]. This mode of operation is also versatile and applicable to any BDFM.

5.4 Doubly-fed asynchronous mode

When both electrical ports are ac supplied, but the synchronous operation is not achieved, the BDFM works in the doubly-fed asynchronous mode, which has also been referred to as double-cascade mode[69]. It occurs in cases where the converter or controller fails to meet the frequency constraint stipulated by (1). The resultant torque characteristic can be predicted as a simple superposition of two cascade induction modes, one supplied at the PW terminal and the other from the CW side, as shown in Fig.12(b). The operating point is determined by the individual torque profiles of both IMs and the load condition.

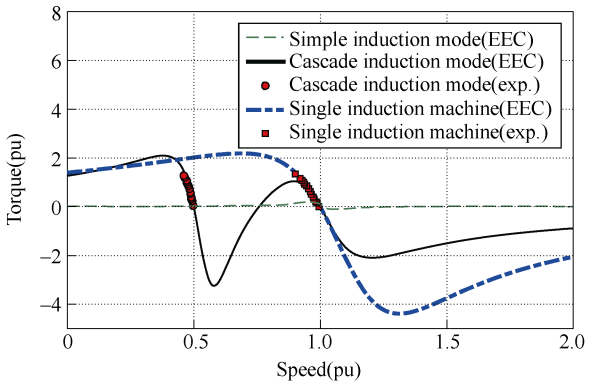

(a) Simple induction mode and cascade induction mode[68]

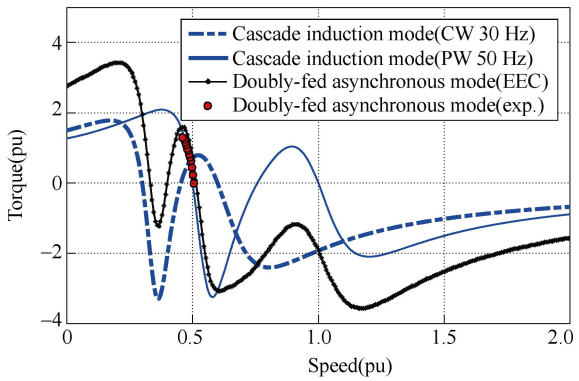

(b) Doubly-fed asynchronous mode[68]

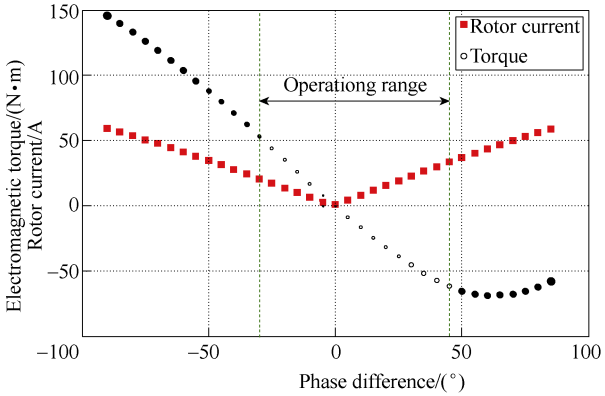

(c) Torque-synchronous angle curve at 1250 r/min[17]

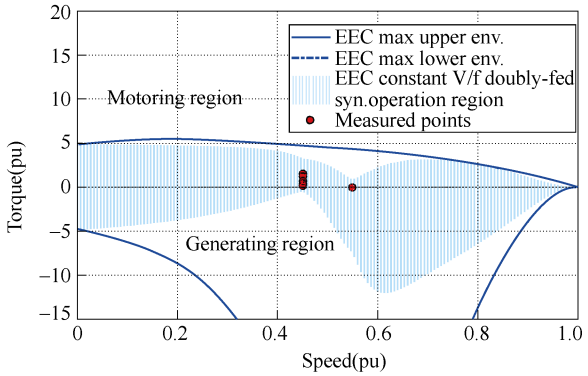

(d) Available operation region in doubly-fed synchronous mode[68]

Fig.12 Torque-speed characteristics of the DS-BDFIM (normalized relative to the PW synchronous speed)

5.5 Doubly-fed synchronous mode

If both electrical ports are supplied from ac sources, and the frequency relationship given by (1) is preserved by the controller, the BDFM is in the doubly-fed

synchronous mode. In this regime, the BDFM performance resembles that of a classical SM and the corresponding torque-angle characteristic is a pure sine-wave offset by dc asynchronous torque components, as shown in Fig.12(c)[17]. The available operation region is outlined in Fig.12(d). It can be seen that the speed-dependent torque capability decreases near the natural and PW synchronous speeds.

There are two complex control variables, i.e., the current and voltage vectors of the PW and/or CW. In principle, either a single-electrical-port control scheme (only one of the electrical ports is actively controlled)[73] or a dual-electrical-port counterpart (both electrical ports are simultaneously regulated)[74-76] can be adopted. In the former option, the PW is usually grid-connected at a constant voltage and frequency, and the CW is supplied from a variable voltage and frequency converter. In the latter case, both the PW and CW are converter-fed. The comparative properties of the two control approaches appear in Table 1.

6 Design considerations

Though the BDFM origins date back to early 1900s, little progress has been made in design methodology until the recent decade, which can be mainly attributed to the obvious distinctions in power flow and operating range between the BDFMs and conventional singly-fed machines. The well-established text-books design methods based on a single airgap volt-ampere rating for traditional dc machines, IMs and SMs are no longer applicable. Therefore, nearly all the early proof-of-concept prototypes, as summarized in [2] and [4], were obtained by rewinding the stator and replacing the rotor of standard IMs. Existing research on the design of BDFMs mainly focus on the modulation type considering their harmonic related issues including torque ripples, time-harmonic distortions, iron saturation, core losses, vibration and acoustic noise, as discussed below.

6.1 Torque ripple and time-harmonic distortion

There will exist a plural of low-order space harmonics mainly due to the asynchronous modulating action of the special rotors in the modulation type if the machine is not well designed. The crowded field harmonics further induce time harmonics in the stator and rotor windings producing undesired distortions of the respective current and voltage waveforms. The frequencies of torque ripples, voltages and currents, which are rotor-speed-dependent, can be well predicted by harmonic analysis[20, 35-36] based on which the commonly-used rotor/stator skewing or tooth notching can be introduced into the BDFIM to substantially reduce the torque ripple and total harmonic distortion (THD) of rotor currents[77].

6.2 Iron saturation

Since the BDFMs are usually used as an adjustable speed constant frequency generator or motor with the converter-fed CW, the variable flux level of the CW is very likely to bring the laminated core into saturation for all BDFMs, especially at the upper band of the speed range[42]. Aside from this operating feature, the modulation type may also suffer from more severe saturation due to the superposition of multiple asynchronous field harmonics. It should be noted that, this saturation phenomenon is usually localized instead of spreading out to the whole magnetic circuit, as pointed out in [78]. The performance considering iron saturation is usually investigated by introducing variable main inductances in the full coupled-circuit model[79] or the steady-state EEC model[44-45]. The saturation effects induce distortions not only of the airgap field distribution but also the torque-angle characteristic. Therefore, they should be taken into account from the original initial sizing to the design optimization stages.

6.3 Core losses

The multi-harmonic feature of the modulation type makes the calculation of core losses much more complex than with the conventional machines. A modified Steinmetz equation is applied for this purpose in the BDFIM to address the issues caused by magnetic fields of different frequencies[41-42,80]. Experimental measurements show that calculations of core loss using the modified Steinmetz equation and core loss curves provided by steel manufacturer generally yield acceptable results, which otherwise will be significantly underestimated by empirical core loss equations for conventional machine design[41,80]. A detailed comparison between a BDFIM and a DFIM of the same power rating and operating range indicates that the core loss of the BDFIM is roughly doubled compared with the DFIM[81]. The obtained core loss results can then be used in EEC models to further predict the steady-state characteristics of the BDFMs by incorporating speed-dependent core loss resistances, as elaborated in Section 4.2.

6.4 Vibration and acoustic noise

The vibration mode of the CDFIM is the same as the DFIM's, but for the modulation type, additional pole-pair-combination-dependent vibration modes

Table 1 Comparison of single-electrical-port and dual-electrical-port control schemes of the BDFM

	Single-electrical-port control[73]	Dual-electrical-port control[74]
Analysis method	Dq-axis theory + field orientation	Spiral vector theory
Control variables	d- and q-axis components of CW current	Circular vectors of PW and CW field current
Slip of rotor winding/Core losses of rotor	Large	Small
Number of current sensor	2 for any two phases of CW (neglecting stator resistance in orientation) or 4 for any two phases of PW and CW (considering stator resistances)	4 for any two phases of PW and CW
Circulating power at low speed?	Yes	No
Rotating coordinate transformation?	Yes	No

always exist[81] even the unbalanced magnetic pull and rotor eccentricity—the main contributors of vibration and noise in conventional machines—are successfully avoided. A larger difference between the PW and CW pole pairs, i.e., far-ratio pole-pair combination, is preferred to avoid low-order vibration levels[82].

7 Control strategies

As mentioned in Section 5.5, the BDFMs can be configured in a single-electrical-port or dual-electrical-port scheme depending on the specific application, yielding two distinct control scenarios. The majority of the existing literature deals with the single-electrical-port control schemes, where the CW voltages and/or currents are directly manipulated to regulate the active and reactive power (grid-connected generation), voltage/ frequency (stand-alone generation) or electro-magnetic torque (grid-connected motoring), so advances in single-electrical-port control are primarily surveyed in this section.

7.1 Sensored control of grid-connected BDFMs

7.1.1 Scalar control

According to (1), the rotor speed can be controlled in an open-loop fashion by simply setting the PW and CW frequencies for the doubly-fed synchronous operation. A standard procedure from the asynchronous start-up to the pull-in synchronization similar to that used for the classical wound-rotor SM is usually required.

By analogy to the slip-ring DFIM operated in doubly-fed synchronous mode, all BDFMs face the open-loop instability problems over most of the potentially useful operating region due to the inherent lack of damping[83]. The open-loop stability analysis has revealed that the stable margin is closely related to both the EEC and mechanical (e.g., inertia and friction coefficient) parameters[84-85] as well as the loading conditions[86]. In order to stabilize BDFMs over the required speed range, closed-loop controllers have to be incorporated.

Owing to its simplicity and relatively low cost of implementation, closed-loop scalar control is the first to be considered. It has been found that, the constant V/f or current control, although by no means optimal, can provide sound performance in a narrow range around the natural synchronous speed for the CDFIM[87], the BDFIM[88], and the BDFRM[89]. The torque can be controlled by adjusting either the CW current[90] or the phase of CW voltage[71] whilst the frequency and V/f ratio are specified in an open-loop manner by synchronous operation constraint.

7.1.2 Field-oriented control

The stator-FOC (SFOC) of the CDFIM in stator-flux reference frame was implemented in [91], and later in [92,93], achieving approximately decoupled active-reactive power control (the active power or speed/torque can be manipulated by the CW q-axis current and the reactive power by the d-axis component) in the desired range around the natural synchronous speed. Cross-coupling between the d-q axes in the outer power/speed loop introduced by the rotor resistive effects was for the first time addressed and compensated for in each axis by PI regulators in [91]. However, little attention had been paid to the cross-coupling between the d-q axes in the inner current loop (introduced by the PW and RW) until [94], where the inner current loop was fully modeled and then simplified to derive a simple but effective feedforward item to improve the stability and dynamic response.

Combined-magnetizing-flux-oriented torque control was implemented in [95], but at the expense of coupled active and reactive power variations. The RFOC was also proposed for the BDFIM in [58] and later used for torque control of the CDFIM with the rated torque sharing ratio to avoid over-rating of one of the two DFIMs[96]. The underlying model was formulated in double (PW and CW)-synchronous reference frames and it was heavily machine-parameter-reliant which significantly reduced the RFOC robustness. It has been revealed that the RFOC and SFOC can provide a fairly consistent response though the former prefers to use amplitude and phase angle as control variables whereas d-q variables are more suitable for the SFOC[73]. Usually two PI stages (e.g. one for the outer power/speed loop and the other for the inner current loop) are required if the CW voltage vector is chosen as a control variable. An enhanced version with an additional PW current PI loop and a simplified one (i.e., single PI) omitting the inner current loop are respectively presented in [61] and[62].

Benefiting from the cage-less rotor and hence fewer machine parameter dependence, the PW real power (or torque in motoring regime) and reactive power control of the BDFRM is inherently decoupled and much simpler relative to its BDFIM companion. The SFOC of the BDFRM, which has similar model equations and control structure as the DFIM despite the fundamentally distinct operating principles, was originally proposed in [97]. The dynamic responses under fixed and/or variable loading conditions were not thoroughly investigated until very recently in [98] and [99], where the influence of PW resistance (i.e., differences between the field and voltage vector orientated control) with reduced machine sizes was for the first time discussed and supported by compelling experimental results.

To date, the only stability study of the closed-loop operation of the BDFM was conducted on the DFIM, considering its similarities with the BDFRM in dynamic model. The study shows that the FOC instability comes from the out-of-sync between the reference frame and stator flux positions. To stabilize the system, either the field orientation process should be fast enough in computation, or a supplementary controller must be designed to compensate for the lack of sufficient system damping for flux fluctuations[86].

7.1.3 Direct control methods

The dynamic vector model also facilitates the development of direct torque control[100] or direct power control (DPC)[101] with sound performance obtained for

the CDFIM using simple switching tables and neglecting the rotor resistance. Under this circumstance, the CDFIM can be treated as a DFIM with modified mutual and leakage inductances. Thus the direct torque control (DTC), and the associated grid synchronization method of DFIM based on the concept of virtual torque (or virtual complex power for DPC), can be readily applied to the CDFIM. A smooth and fast synchronization can be achieved without inrush currents, no PLL, PI regulators or rotor position/speed information normally required by the FOC[102], as demonstrated in [100] and [103].

A so-called predictive DTC for the BDFIM, employing PI controllers and a pulse-width-modulated (PWM) inverter was proposed in [104] as an alternative to the commonly-used DTC with hysteresis comparators. The classical switching-table-based hysteresis DTC was implemented on the BDFIM in [105], but with degraded performance experienced even at a fast sampling rate (100μs), mainly due to the non-optimal prototype design abundant in spatial harmonics[51].

By the absence of the rotor windings, the DTC for the BDFRM can largely inherit from that of the slip-ring DFIM, as demonstrated in [106] (i.e. the switching-table-based) and [107] (i.e. with space vector PWM). An improved DTC technique with indirect stator-quantities control (ISC) for the BDFIM was proposed to eliminate the complex rotating coordinate transformations (i.e. the CW flux components should be estimated in, or converted to, a stationary frame for the sector detection) and reduce the parameter dependence(as both the CW flux and torque estimation involve inductances)[108-109].

Apart from the considered field-oriented control and direct control methods, a robust control algorithm based on the integral sliding mode control (SMC) for the BDFIM was proposed to eliminate the speed error and compensate the system uncertainties caused by the rotor flux and parameter variations, while achieving the approximately decoupled control of rotor speed and reactive power[110]. Another super-twisting sliding mode direct power control was proposed to lower the power ripple and THDs of the PW and CW currents[111]. Model predictive control (MPC) has also been proposed for the BDFMs recently[112]. The feedback linearization (FBL) has been applied to the BDFIM, yet suffering from sensitivity issues[2].

7.1.4 Control strategies under unbalanced or grid fault conditions

In grid-connected applications, the BDFM is required to have the ability to mitigate the adverse effects of unbalanced or even distorted network conditions. A control scheme based on power compensation under unbalanced grid conditions was proposed for DPC of the CDFIM to eliminate the negative-sequence components of the PW currents and to improve the power quality[101]. A dual PI vector control algorithm in two synchronous reference frames for the BDFIM was put forward to regulate the positive-sequence components for control of active and reactive power, and the negative counterparts for other control targets[113]. The further dynamic performance boost was accomplished using a proportional integral resonant (PI+R) controller in a single synchronous reference frame[114].

With respect to the LVRT, it has been reported that the CDFIM and BDFIM exhibit milder transients relative to the DFIM regarding the currents, DC-link voltage, electro-magnetic torque and turbine speed under serious voltage dips[115], showing greater potential for grid code compliance. Crowbar-less LVRT of the BDFIM has been demonstrated to be feasible for both symmetrical and asymmetrical faults[116-117], owing to the inherently larger rotor leakage inductance effectively limiting the CW current levels during voltage transients. However, the increased rotor leakage inductance makes it difficult for the machine side converter (MSC) to control the PW reactive power[118], indicating that further measures are still necessary in this direction to allow the BDFIM to fully satisfy the grid integration requirements[119]. A crowbar or a series dynamic resistor commonly used in conventional DFIM systems[120] and an improved LVRT control strategy based on the flux linkage tracking[121] are suggested for this purpose.

7.2 Sensored control of stand-alone BDFM system

Vector control with CW current orientation is widely used to stabilize the output voltage amplitude and frequency of BDFM-based stand-alone power generation systems regardless of the varying rotor speed and loading conditions[122-130]. The CW-current-oriented control with simplified dual-closed-loop scheme(i.e., outer voltage/frequency loop and inner current loop) was first presented in [122]. However, unexpected fluctuations in the output voltage amplitude were observed with IM loads and a compensation strategy based on synchronous sampling and harmonic injection was proposed in [123]. Other control options, i.e., with CW voltage and/or flux alignment were modeled and compared with CW current oriented control in [124].

The cross-coupling effects between the d-q axes in the inner current loop(introduced by the PW and RW) observed within grid-connected BDFM systems also appear in stand-alone applications, slowing down the transient response of the output voltage. Commonly-used feedforward approaches[125] and a new decoupling network method[126] have been implemented for this reason. A frequency-domain method based on numerical calculation of transfer functions was proposed to better design the voltage and current PI regulators, which has provided fast dynamic performance without the need for feedforward terms[127]. Unbalanced and low-order harmonic voltages arising from non-linear loads can be suppressed by injecting harmonic current components into the CW[128].

The line side converter(LSC) can also be fully used to alleviate the load disturbance implications, although only balanced and linear loads have currently been considered, and thus enhance the voltage quality of the point-of-common coupling(PCC) (i.e., where the LSC and PW are connected) through control of LSC reactive current[129]. DC-link current feedforward is suggested to stabilize the DC-link voltage and speed up the LSC dynamic response[130].

7.3 Sensorless control

At present, the sensorless control of the BDFMs is lagging far behind its DFIM counterpart, primarily due to the model complexity and/or the strong parameter dependence. To date, the BDFRM has achieved more than satisfactory sensorless operation[106, 131-136]. A low-cost position sensorless control scheme for the BDFRM was first realized by affecting the torque angle in a closed-loop manner, while the speed command is implicated in the rotational angle used for coordinate transformations[131]. An encoder-less DTC scheme was proposed for speed regulation in [106], but the flux estimation suffered from high sensitivity to inductance knowledge uncertainties in real-time implementation. By replacing the CW flux with reactive power as the control variable, the nearly parameter-independent (only the PW resistance used) torque and reactive power control is realized. However, for speed control, either a shaft encoder or a rotor speed observer is still required[132]. Instead of using the torque and flux as control variables, which are more susceptible to estimation errors, the measurable active and reactive power are directly controlled in[133]. The performance is improved in comparison to methods used in [106] and[132] owing to the use of active voltage vectors only and a CW-flux-independent sector identification technique. Recently, a sensorless FOC scheme for speed regulation has been developed to address the variable switching frequency and flux (torque) ripple issues of the original encoder-less DTC[134]. Model reference adaptive systems (MRASs) with CW flux and reactive power control were implemented in [135] and [136] respectively to estimate the rotor speed, indicating good speed tracking abilities of the controller.

Sensorless control of the BDFIM was first implemented using a modified EEC model derived from the standard configuration shown in Fig.11(a) to separate the magnetizing and torque-producing current components by referring the PW and RW leakage inductance terms to the CW side[137]. However, the usual CW terminal voltage integration used to estimate the respective flux vector is highly inaccurate near the natural synchronous speed. It is caused by the well-known adverse effects of resistance variations at low supply voltages. A MRAS observer based on the CW current and a rotor speed estimator was proposed to achieve sensorless control of rotor speed[138].

Sensorless stand-alone generating operation of the BDFM has also drawn increasing attention recently. Based on the voltage control scheme discussed in Section 7.2, the PW q-axis voltage was regulated to estimate the CW frequency, and the rotor speed can then be immediately obtained from (1)[139]. The new speed observer based on a rotor position PLL and a second-order generalized integrator was implemented for different loads in [140].

7.4 Control comparisons of BDFM and DFIM

Given the inductances are constant, there will be two more cross-couplings between the d-q axes in the BDFIM and CDFIM imposed by the rotor resistance, one for each control loop(outer and inner for currents). It has been found that, in the case of outer power/speed control loop, this can be quantitatively measured by a dimensionless number σ—the product of the slip frequency and transient time constant of the rotor, which can be expressed as follows:

$$\sigma = \frac{\left(\omega_{\mathrm{p}} - p_{\mathrm{p}}\omega_{\mathrm{r}}\right)\left(L_{\mathrm{r}} - L_{\mathrm{mp}}^2 / L_{\mathrm{sp}}\right)}{R_{\mathrm{r}}} \tag{3}$$

The larger σ is, the weaker the cross-coupling between the axes will be, and the better decoupled control can be achieved[73,92]. If σ is big enough, then ignoring the rotor resistance will result in a DFIM-like control property of the BDFM. Parameters and calculated σ values at 0.7 and 1.3 times the natural synchronous speed($\sigma_{0.7}$ and $\sigma_{1.3}$ respectively) are tabulated in Table 2. It can be seen that, the rotor transient time constant is heavily reliant on the machine design. However, the pole pair combination plays a more significant role in the σ magnitude. Generally, $p_{\mathrm{p}} < p_{\mathrm{c}}$ (for the BDFIM) and $p_{\mathrm{p}}=p_{\mathrm{c}}$(for the CDFIM) yield larger σ values. A larger σ indicates a better control property similar to the DFIM's within the desired speed range(±30% natural synchronous speed), but a slight increase in rotor core losses can be expected. The cross-coupling between *dq* axes in inner current loop is usually compensated by a series of feedforward terms.

Table 2 Comparison of cross-coupling of different BDFMs between dq axes in outer control loop

Parameters and calculated values	CDFIM[93]	BDFIM[108]	CDFIM[92]	BDFIM[62]	BDFIM[51]	BDFRM[98]
Pole pair combination $p_{\mathrm{p}}/p_{\mathrm{c}}$	2/2	3/1	2/2	2/4	1/3	3/1
PW self-inductance L_{sp}/mH	53.5	292	87.14	349.8	714.8	410
PW-RW mutual inductance L_{mp}/mH	50	2.16	85	3.1	242.1	-
CW-RW mutual inductance L_{mc}/mH	50	4	85	2.2	59.8	-
RW self-inductance L_{r}/mH	107	0.048	174.28	4.452×10^{-2}	132.6	-
RW resistance R_{r}/Ω	1.4	1.73×10^{-4}	0.41	1.297×10^{-4}	0.473	0
Rotor circuit transient time constant $(L_{\mathrm{r}}-L_{\mathrm{mp}}^2/L_{\mathrm{sp}})/R_{\mathrm{r}}$ (s)	0.0431	0.1851	0.2228	0.1314	0.1070	inf
PW/natural synchronous speed /(r/min)	1800/900	1000/750	1500/750	1500/500	3000/750	1000/750
Rotor slip at the top speed (1.3 times natural synchronous speed)	0.35	0.025	0.35	0.567	0.675	0.025
$\sigma_{1.3}$	5.687	1.454	24.498	23.392	22.690	+inf
Rotor slip at the bottom speed (0.7 times natural synchronous speed)	0.65	0.475	0.65	0.767	0.825	0.475
$\sigma_{0.7}$	10.561	27.622	45.497	31.648	27.732	+inf
Investigated speed range (p.u.) (normalized relative to ω_{n})	−0.5-(+0.26)	−0.33-(+0.31)	−0.2-(+0.2)	−0.3-(+0.1)	−1.0-(+1.0)	−0.2-(+0.2)
Is R_{r} neglected in implementation?	Yes	No	Yes	Yes	Yes	-

An inductor-capacitor(LC) filter is usually installed between the MSC and the CW to eradicate the high-frequency PWM voltage harmonics since BDFMs are more sensitive to harmonic contamination[125] compared with the DFIM. Current hysteresis PWM and classical DTC prohibit the use of filter and the quality of output voltage at PW terminal will be seriously deteriorated in stand-alone systems.

8 Concluding remarks and future trends

Based on the systematic review of the existing BDFMs in terms of topology, operating principles, modeling, control and applications, it is found that though highly-reliable and cost-effective, BDFMs generally feature relatively lower torque/power density, inferior efficiency and harmonic-related issues (for the modulation type) compared with the conventional DFIM. This is largely due to the fact that they employ indirect magnetic coupling instead of directly using fundamental flux/field components to realize the slip power transfer. The torque/power density may be elevated to the level on a par with standard industrial IMs by further design optimization as demonstrated in [39] and [42]. The efficiency can also be improved by more optimal design or introducing reactive compensation devices at PCC[42,141]. The most challenging part may lie in the mitigation of harmonic-related issues (e.g., additional losses, lower output power quality, vibration and acoustic noise) inherited from the multi-harmonic nature of the modulation type especially under heavy or even overload conditions, though they can be alleviated to some extent by sophisticated design and control techniques, such as the work done in [82, 113, 114] and [123]. As a consequence, the development of a successful BDFM-based system is faced with a number of tradeoffs between:

- The torque/power density and the efficiency[39, 42].
- The power factor (or reactive power capability) of the PW and the volt-ampere rating of the MSC supplying the CW[141-143].
- The torque density and vibration behavior in the selection of suitable pole-pair combination[81, 144].
- The control property and rotor core losses (or efficiency) in determining the rated operating point[45].
- The PW reactive power capability and the LVRT performance in design of rotor leakage inductance for grid-connected wind power applications[118-119].
- The electromagnetic performance and manufacturing cost[26, 145].

The above compromises pose tough challenges on the design of the BDFM-based systems, which means the points of concern in design stage should be addressed according to specific applications since not all the desired performance indexes can be simultaneously achieved. In addition, the rotor structure, including the pole pair combination[78,144] and detailed geometrical variations[146] which primarily affect the similarity between the practical rotor construction and the idealized airgap field modulator, have been demonstrated to have significant influence on the performance of BDFMs. Therefore the rotor design and manufacture is crucial and optimization on a multi-objective basis is necessary.

With respect to the modeling methods, the harmonic analysis proves to be rather effective for explaining the operating principle of the BDFIM. Steady-state analysis relies on the per-phase EEC, while the dynamic performance is usually studied by two-axis or space vector models. These methods are quite time-saving with acceptable accuracy. However, for higher accuracy, FE methods are more appealing. Special features of BDFM rotors, such as the self-closed rotor circuit (CDFIM and BDFIM), axial lamination or thin rib (BDFRM), etc., unavoidably complicate the FEA and under most circumstances, fine meshing and time-consuming time-stepping FE analysis are required. MEC[40-42], computationally efficient FE methods[43] and semi-analytical methods[147], for population-based design optimizations are meaningful explorations in this direction.

Thanks to the past decade's exhaustive research, all available functional modes of BDFMs have been identified. However, little attention has been paid to the utilization of other operating modes except for the doubly-fed synchronous operation and transitions between them, which shows promise in fail-safe post-fault conditions.

Substantial knowledge has been gained on control aspects. A detailed qualitative comparison of various control methods reviewed in Section 7 is listed in Table 3. It can be seen that FOC for sensored grid-connected applications and voltage control for stand-alone BDFM systems (sensored or sensorless) have the highest technical maturity, and are the mainstream for the time being. In both control strategies, the cross-coupling phenomena between dq axes in the power/speed and/or current loops coming from resistive effects have been extensively investigated, and several new methods proposed and implemented to achieve satisfactory decoupled control. In contrast to FOC, the DT(P)C is a rather competitive alternative for sensorless control of the BDFMs. Developing robust control schemes for BDFMs with superior immunity to parameter variations and disturbances is the next step, as pioneered by the recent research work in [108, 126, 133].

Advantages and limitations of the prevailing BDFM topologies have been identified and compared with the established DFIM as tabulated in Table 4. It can be seen that peculiarities of the BDFM result in distinct differences from the more traditional singly-fed machines and slip-ring DFIM in design, analysis, control and even manufacturing. Advances in the field of the BDFM have already been an indispensable complement and invaluable contribution to the existing theories of electric machinery. For instance, the general airgap field modulation theory proposed in [5] was based on the development of BDFMs.

In contrast, the practical application of BDFMs has been greatly challenged mainly due to its relatively low torque/power density and efficiency compared with the conventional singly-fed machines and slip-ring doubly-fed machines. To date, several large BDFMs have been prototyped as the milestones on the way to practical

Table 3 Comparison of control methods of the BDFM

Metrics of interest	Scalar control		FOC	FBL	SMC	ISC	DT(P)C (classical)	MPC	Voltage control
	Open-loop	Closed-loop							
Need rotating coordinate transformation?	No	No	Yes	Yes	Yes	No	Yes	Yes	No
Need PWM modulator?	Yes	Yes	Yes	Yes	Yes	Yes	No	No	Yes
Computational burden	Low	Low	Heavy	Heavy	Heavy	Heavy	Low	Heavy	Low
Sensitivity to parameter changes and disturbance	Low	Low	High	High	Low	Low	High	High	Low
Dynamic response	Slow	Slow	Fast	Fast	Fast	Fast	Fast	Fast	Fast
Sensorless operation realized?	[88]	[131]	[134, 137]	No	No	No	[132-133]	No	[139]
Need parameter tuning?	No	Yes	Yes	Yes	Yes	Yes	No	No	Yes
Flux/torque/power ripple	large	Large	Low	Low	Small	Low	Large	Small	-
Stability	Local stable		Dependent on controller parameters					Stable	
Cost	Low	Low	High	High	High	High	Low	High	Low
Technical maturity	High	High	High	Low	Low	Low	Low	Low	High

Table 4 Comparison of conventional DFIM and various emerging BDFM technologies for ±30% limited speed range applications

Topology	DFIM[12,81,141]	CDFIM[12,17,56,91]	DFIM-RT[7]	BDFIM (wound rotor)[22,25]	BDFIM (nested-loop rotor)[8,12,31]	BDFRM[9,30,31,65,98,143]	BDFM with hybrid rotor[10]
Speed range	$\pm 0.3\omega_p$	$\pm 0.3\omega_n$ ($<\omega_p/p_p$)	$\pm 0.3\omega_p$ ($\neq\omega_p$)	$\pm 0.3\omega_n$ ($<\omega_p/p_p$)	$\pm 0.3\omega_n$ ($<\omega_p/p_p$)	$\pm 0.3\omega_n$	$\pm 0.3\omega_n$
Torque density	+ + +	+ + −	+ + −	+ + −	+ + −	+ + −	+ + −
Efficiency	+ + +	+ − −	+ − −	+ − −	+ + −	+ + +	+ + −
Torque ripple	+ + +	+ + +	+ + +	− − −	− − −	− − −	− − −
Power quality	+ + +	+ + +	+ + +	+ + −	+ + −	+ + −	+ + −
React. power capability	+ + +	+ + −	+ + +	+ + −	+ − −	+ − −	+ − −
Modeling and analysis	+ + +	+ + −	+ + +	+ + −	+ − −	+ + −	− − −
Control property	+ + +	+ − −	+ + −	+ + −	+ + −	+ + +	+ + −
Vibration and noise	+ + +	+ + +	+ + +	+ + −	+ + −	+ + −	+ + −
Mechanical reliability	− − −	+ − −	+ − −	+ − −	+ + −	+ + +	+ + −
Maintenance cost	− − −	+ + +	+ + +	+ + +	+ + +	+ + +	+ + +
High-speed operation	− − −	− − −	− − −	− − −	+ + −	+ + +	+ + −
LVRT capability	− − −	+ + +	+ + +	+ + +	+ + +	+ + +	+ + +
Ease of manufacture	+ + +	+ + +	+ + +	+ + −	+ + −	+ − −	− − −
Technical maturity	+ + +	+ + −	− − −	+ + −	+ + −	+ + −	− − −

deployment of BDFMs for wind energy conversion systems (e.g., the 90kW DFIM-RT[7], the 200kW BDFRM[145] and the 250kW BDFIM[116]) or ship shaft power generation (e.g., the 64kW wound rotor BDFIM[129]). With the irreplaceable virtues of unique variable speed constant frequency characteristics, robust construction, fail-safe operating nature, and flexible power flow, in addition to the technically demonstrated pump drives and wind turbines, the BDFMs may also play an important role in some safety-critical applications where the performance of the conventional singly-fed machines will unavoidably be compromised by the fault-tolerant design techniques, such as motors/ generators for variable-frequency ac aerospace networks.

References

[1] B. Hopfensperger, and D. J. Atkinson, "Doubly-fed a.c. machines: classification and comparison, " *Proc. Eur. Power Electron. Drives,* Graz, Austria, pp. 1-17, 2001.

[2] P.C. Roberts, *A Study of Brushless Doubly-Fed (Induction) Machines*. Ph.D. thesis, Cambridge, U. K.:Univ. Cambridge, 2004.

[3] M.G. Jovanović, "Sensored and sensorless speed control methods for brushless doubly fed reluctance motors," *IET Electr. Power Appl.*, vol.6, no.3, pp. 503-513, 2009.

[4] F. Zhang, S. Yu, and H. Wang, "Overview of research and development status of brushless doubly-fed machine system," *Ch. J. Electr. Eng*., vol.2, no.2, pp.1-13, 2016.

[5] M. Cheng, P. Han, and W. Hua, "A general airgap field modulation theory for electrical machines," *IEEE Trans. Ind. Electron*., vol.64, no.8, pp. 6063-6074, 2017.

[6] L. J. Hunt, "A new type of induction motor," *Proc. IEE*, vol.39, no.186, pp. 648-667, 1907.

[7] M. Ruviaro, F.Runcos, N. Sadowski, and I. M. Borges, "Analysis and test results of a brushless doubly-fed induction machine with rotary transformer," *IEEE Trans. Ind. Electron*., vol.59, no.6, pp. 2670-2677, 2012.

[8] A. R. W. Broadway, and L. Burbridge, "Self-cascaded machine: a low speed motor or high frequency brushless alternator," *Proc. IEE*, vol.117, no.7, pp. 1277-1290, 1970.

[9] A. R. W. Broadway, "Cageless induction machine," *Proc. IEE*, vol.118, no.11, pp.1593-1600, 1971.

[10] F. Zhang, G. Jia, Y. Zhao, Z, Yang, and W. Cao, "Simulation and experimental analysis of a brushless electrically excited synchronous machine with hybrid rotor," *IEEE Trans. Mag*., vol.51, no.12,pp.1-7, Article #: 8115007, 2015.

[11] S. Abdi, E. Abdi, A. Oraee, and R. McMahon, "Optimization of magnetic circuit for brushless doubly fed machines," *IEEE Trans. Energy Convers*., vol.33, no.4, pp. 1611-1620, 2015.

[12] R. A. McMahon, P. C. Roberts, X. Wang, and P. J. Tavner, "Performance of BDFM as generator and motor," *IEE Electr. Power Appl.*, vol.153, no.2, pp. 289-299, 2006.

[13] D. C. Ludois, J. K. Reed, and K. Hanson, "Capacitive power transfer for rotor field current in synchronous machines, " *IEEE Trans. Power Electron*., vol.27, no.11, pp. 4638-4645, 2012.

[14] N. U. R. Malik, and C. Sadarangani, "Brushless doubly-fed induction machine with rotating power electronic converter for power applications," *Proc. Int. Conf. Electr. Mach. Syst*., Beijing, China, pp. 1-6, Aug. 2011.

[15] B. H. Smith, "Synchronous behavior of doubly fed twin stator induction machine," *IEEE Trans. Power Apparat. Syst*., vol.PAS-86, no.10, pp. 1227-1236, 1967.

[16] B. Hopfensperger, D. J. Atkinson, and R. A. Lakin, "Steady state of the cascaded doubly-fed induction machine," *Eur. Trans. Electr. Power*, vol.12, no.6, pp. 427-437, 2002.

[17] P. Han, M. Cheng, and R. Luo, "Design and analysis of a brushless doubly-fed induction machine with dual-stator structure," *IEEE Trans. Energy Convers.*, vol.31, no.3, pp. 1132-1141, 2016.

[18] S. Abdi, E. Abdi, and R. A. McMahon, "A study of unbalanced

magnetic pull in brushless doubly fed machines," *IEEE Trans. Energy Convers*., vol.30, no.3, pp. 1218-1227, 2015.

[19] L. Han, X. Ou, J. Du, X. Han, and Y. Guo, "Study of direct coupling in stator dual windings of brushless doubly-fed machine," *IEEE Trans. Energy Convers*., vol.32, no.3, pp. 974-982, 2017.

[20] S. Williamson, A. C. Ferreira, and A. K. Wallace, "Generalised theory of the brushless doubly-fed machine. part 1: analysis, " *IEE. Proc.-Electr. Power Appl.*, vol.144, no.2, pp.111-121, 1997.

[21] H. Gorginpour, B. Jandaghi, and H. Oraee, "A novel rotor configuration for brushless doubly-fed induction generators," *IET Electr. Power Appl*., vol.7, no.2, pp. 106-115, 2013.

[22] F. Xiong, and X. Wang, "Design of a low-harmonic-content wound rotor for the brushless doubly fed generator," *IEEE Trans. Energy Convers*., vol.29, no.1, pp. 158-168, 2014.

[23] R. A. McMahon, P. Tavner, E. Abdi, P. Malliband, and D. Barker, "Characterising brushless doubly fed machine rotors," *IET Electr. Power Appl*., vol.3, no.7, pp. 535-543, 2013.

[24] A. Oraee, E. Abdi, S. Abdi, R. McMahon, and P. J. Tavner, "Effects of rotor winding structure on the BDFM equivalent circuit parameters, " *IEEE Trans. Energy Convers*., vol.30, no.4, pp. 1660-1669, 2015.

[25] L. Jia, and X. Wang, "A comparison of the wound rotor and nested?loop rotor brushless doubly fed generator, " *IEE J. Trans. Electr. Electron. Eng.*, vol.12, no.2, pp. 273-283, 2017.

[26] S. Williamson, and M. S. Boger, "Impact of inter-bar currents on the performance of the brushless doubly fed motor," *IEEE Trans. Ind. Appl*., vol.35, no.2, pp. 453-460, 1999.

[27] Y. Liao, L. Xu, and L. Zhen, "Design of a doubly fed reluctance motor for adjustable-speed drives," *IEEE Trans. Ind. Appl*., vol.32, no.5, pp.1195-1203, 1996.

[28] I. Scian, D. G. Dorrell, and P. J. Holik, "Assessment of losses in a brushless doubly-fed reluctance machine," *IEEE Trans. Magn*., vol.42, no.10, pp.3425-3427, 2006.

[29] T. Fukami, M. Momiyama, and K. Shima, "Steady-state analysis of a dual-winding reluctance generator with a multiple-barrier rotor," *IEEE Trans. Energy Convers*., vol.23, no.2, pp.492-498, 2008.

[30] L. Xu, Y. Tang, and L. Ye, "Comparison study of rotor structures of doubly excited brushless reluctance machine by finite element analysis," *IEEE Trans. Energy Convers*., vol.9, no.1, pp.165-172, 1994.

[31] L. Xu, and F. Wang, "Comparative study of magnetic coupling for a doubly fed brushless machine with reluctance and cage rotors," *Rec. Ind. Appl. Soc. Annu. Meeting*, New Orleans, LA, USA, pp. 326-332, Oct. 1997 .

[32] E. Schulz, and R. E. Betz, "Optimal rotor design for brushless doubly fed reluctance machines," *Rec. Ind. Appl. Soc. Annu. Meeting*, Salt Lack City, USA, pp. 256-261, Oct. 2003 .

[33] S. Khaliq, M. Modarres, T. A. Lipo, and B. I. Kwon, "Design of novel axial flux dual stator doubly fed reluctance machine," *IEEE Trans. Magn*., vol.51, no.11, pp.1-4, 2015.

[34] F. Zhang, L. Zhu, S. Jin, X. Su, S. Ademi, and W. Cao, "Controller strategy for open-winding brushless doubly-fed wind power generator with common mode voltage elimination," *IEEE Trans. Ind. Electron*., vol.PP, no.99, DOI: 10.1109/ TIE.2018.2811370, 2018.

[35] F. Blázquez, C. Veganzones, and D. Ramírez, "Characterization of the rotor magnetic field in a brushless doubly-fed induction machine," *IEEE Trans. Energy Convers*., vol.24, no.3, pp. 599-607, 2009.

[36] X. Chen, and X. Wang, "Proximate standing wave feature of magnetic field and its influence on the performance of wound rotor brushless doubly-fed machine," *IEEE Trans. Energy Convers*., vol.32, no.1, pp. 296-308, 2017.

[37] A. C. Ferreira, and S. Williamson, "Time-stepping finite-element analysis of brushless doubly fed machine taking iron loss and saturation into account," *IEEE Trans. Ind. Appl*., vol.35, no.3, pp. 583-588, 1999.

[38] H. Gorginpour, H. Oraee, and R. A. McMahon, "Performance description of brushless doubly-fed induction machine in its asynchronous and variable speed synchronous modes," *J. Electromag. Analy. Appl*., vol.3, no.12, pp.490-511, 2011.

[39] P. Han, M. Cheng, Y. Jiang, Z. Chen, "Torque/power density optimization of a dual-stator brushless-doubly-fed induction generator for wind power application," *IEEE Trans. Ind. Electron*., vol.64, no.2, pp. 9864-9875, 2017.

[40] M. Hsieh, I. H. Lin, and D. G. Dorrell, "Magnetic circuit modeling of brushless doubly-fed machines with induction and reluctance rotors," *IEEE Trans. Magn*., vol.49, no.5, pp. 2359-2362, 2013.

[41] H. Gorginpour, H. Oraee, and R. A. McMahon, "A novel modeling approach for design studies of brushless doubly fed induction generator based on magnetic equivalent circuit," *IEEE Trans. Energy Convers*., vol.28, no.4, pp. 902-912, 2013.

[42] H. Gorginpour, H. Oraee, and R. A. McMahon, "Electromagnetic-thermal design optimization of the brushless doubly fed induction generator," *IEEE Trans. Ind. Electron*., vol.61, no.4, pp. 1710-1721, 2014.

[43] X. Wang, T. D. Strous, D. Lahaye, H. Polinder, and J. A. Ferreira, "Modeling and optimization of brushless doubly-fed induction machines using computationally efficient finite-element analysis," *IEEE Trans. Ind. Appl*., vol.52, no.6, pp. 4525-4534, 2016.

[44] N. Chilakapati, V. S. Ramsden, and V. Ramaswamy, "Investigation of doubly fed twin stator induction motor as a variable speed drive, " *Proc. Int. Conf. Power Electron. Drives Energy Syst. Ind. Growth*, Perth, Australia, pp. 160-165, Dec. 1998.

[45] P. Han, M. Cheng, X. Wei, and Y. Jiang, "Steady-state characteristics of the dual-stator brushless doubly-fed induction generator," *IEEE Trans. Ind. Electron.*, vol.65, no.1, pp. 200-210, 2018.

[46] P. C. Roberts, R. A. McMahon, P. J. Tavner, "Equivalent circuit for the brushless doubly fed machine (BDFM) including parameter estimation and experimental verification, " *IEE Electr. Power Appl*., vol.152, no.4, pp. 933-942, 2005.

[47] S. Tohidi, "Analysis and simplified modelling of brushless doubly-fed induction machine in synchronous mode of operation," *IET Electr. Power Appl.*, vol.10, no.2, pp. 110-116, 2016.

[48] M. Hashemnia, F. Tahami, and E. Oyarbide, "Investigation of core loss effect on steady-state characteristics of inverter fed brushless doubly fed machines," *IEEE Trans. Energy Convers*., vol.29, no.1, pp. 57-64, 2014.

[49] S. Abdi, E. Abdi, A. Oraee, and R. McMahon, "Equivalent circuit parameters for large brushless doubly fed machines (BDFMs)," *IEEE Trans. Energy Convers.*, vol.29, no.3, pp. 706-715, 2014.

[50] R. A. McMahon, P. C. Roberts, M. Tatlow, and E. Abdi, "Rotor parameter determination of the brushless doubly fed (induction) machine," *IET Electr. Power Appl*., vol.9, no.8, pp. 549-555, 2015.

[51] J. Poza, *Modélisation, Conception et Commande d'une Machine Asynchrone sans Balais Doublement Alimentée pour la Génération à Vitesse Variable*. Ph.D. thesis, France:Institut National Polytechnique de Grenoble, 2003.

[52] A. Ramchandran, G. C. Alexander, "Frequency-domain parameter estimation for the brushless doubly-fed machine," *Proc. Power Convers. Conf.*, Yokohama, Japan, pp. 346-351, Apr. 1993.

[53] H. Djadi, K. Yazid, M. Menaa, "Parameters identification of a brushless doubly fed induction machine using pseudo-random binary signal excitation for recursive least squares method," *IET Electr. Power Appl*., vol.11, no.9, pp. 1585-1595, 2017.

[54] J. Su, Y. Chen, L. Sun, X. Liu, and Y. Kang, "Parameter estimation of brushless doubly-fed induction generator based on steady experimental results," *Proc. IEEE Energy Convers. Congr. Expo.*, Montreal, Canada, Sep. pp. 2800-2804, 2015.

[55] D. Gay, R. Betz, D. G.Dorrell, and A. M. Knight, "Brushless doubly fed reluctance machine parameter determination," *Proc. Int. Conf. Electr. Mach. Syst.,* Sydney, Australia, pp.1-6, Aug.2017.

[56] G. Esfandiari, M. Ebrahimi, A. Tabesh, and M. Esmaeilzadeh, "Dynamic modeling and analysis of cascaded DFIMs in an arbitrary reference frame," *IEEE Trans. Energy Convers*., vol.30, no.3, pp.999-1007, 2015.

[57] R. Li, A. K.Wallace, and R. Spée, "Two-axis model development of cage rotor brushless doubly-fed machines, " *IEEE Trans. Energy Convers*., vol.6, no.3, pp.453-460, 1991.

[58] D. Zhou, R. Spée, and G. C. Alexander, "Experimental evaluation of a rotor flux oriented control algorithm for

brushless doubly-fed machines," *IEEE Trans. Power Electron*., vol.12, no.1, pp. 72-78, 1997.

[59] M. S. Boger, A. K.Wallace, and R. Spée, "General pole number model of the cage-rotor brushless doubly-fed machine," *IEEE Trans. Ind. Appl.*, vol.31, no.5, pp.1022-1028, 1995.

[60] P. C. Roberts, T. Long, and R. A. McMahon,"Dynamic modelling of the brushless doubly fed machine," *IET Proc. -Electr. Power Appl*., vol.7, no.7, pp. 544-556, 2013.

[61] J. Poza, E. Oyarbide, and I. Sarasola, "Vector control design and experimental evaluation for the brushless doubly fed machine, " *IET Proc.-Electr. Power Appl.*, vol.3, no.4, pp. 247-256, 2009.

[62] S. Shao, E. Abdi, and F. Barati, "Stator-flux-oriented vector control for brushless doubly fed induction generator," *IEEE Trans. Ind. Electron*., vol.56, no.10, pp. 4220-4228, 2009.

[63] F. Barati, S. Shao, E. Abdi, H. Oraee, and R. McMahon, "Generalized vector model for the brushless doubly-fed machine with a nested-loop rotor,"*IEEE Trans. Ind. Electron*., vol.58, no.6, pp.2313-2321, 2011.

[64] F. Liang, L. Xu, and T. A. Lipo, "D-q analysis of a variable speed doubly ac excited reluctance motor," *Electr. Mach. Power Syst*., vol.19, no.2, pp.125-138, 1990.

[65] L. Xu, F. Liang, and T. A. Lipo, "Transient model of a doubly excited reluctance motor, " *IEEE Trans. Energy Convers*., vol.6, no.1, pp. 126-133, 1991.

[66] R. E. Betz, and M. G. Jovanović, "Introduction to the space vector modelling of the brushless doubly-fed reluctance machine," *Electr. Power Compon. Syst*., vol.31, no.8, pp. 729-755, 2003.

[67] N. Patin, E. Monmasson, and J. Louis, "Modeling and control of a cascaded doubly fed induction generator dedicated to isolated grids," *IEEE Trans. Ind. Electron*., vol.56, no.10, pp. 4207-4219, 2009.

[68] P. Han, M. Cheng, X. Wei, and N. Li, "Modeling and performance analysis of a dual-stator brushless doubly fed induction machine based on spiral vector theory," *IEEE Trans. Ind. Appl*., vol.52, no.2, pp.1380-1389, 2016.

[69] S. Tohidi, M. Zolghadri, H. Oraee, and P. Tavner, "Performance of the brushless doubly-fed machine under normal and fault conditions,"*IET Electr. Power Appl.*, vol.6, no.9, pp. 621-627, 2012.

[70] F. Wang, F. Zhang, and L. Xu, "Parameter and performance comparison of doubly fed brushless machine with cage and reluctance rotors," *IEEE Trans. Ind. Appl*., vol.38, no.5, pp.1237-1243, 2002.

[71] S. Shao, E. Abdi, and R. A. McMahon, "Low-cost variable speed drive based on a brushless doubly-fed motor and a fractional unidirectional converter," *IEEE Trans. Ind. Electron*., vol.59, no.1, pp. 317-325, 2012.

[72] M. Kong, X. Wang, Z. Li, and P. Nie, "Asynchronous operation characteristics and soft-starting method for the brushless doubly-fed motor," *IET Electr. Power Appl*., vol.11, no.7, pp. 1276-1283, 2017.

[73] P. Han, M. Cheng, and Z. Chen, "Single-electrical-port control of cascaded doubly-fed induction machine for EV/HEV applications," *IEEE Trans. Power Electron.*, vol.32, no.9, pp. 7233-7243, 2017.

[74] P. Han, M. Cheng, and Z. Chen, "Dual-electrical-port control of cascaded brushless doubly-fed induction drive for EV/HEV applications," *IEEE Trans. Ind. Appl*., vol.53, no.2, pp.1390-1398, 2017.

[75] R. S. Rebeiro, and A. M. Knight, "Two converter based operation of a brushless doubly fed reluctance machine, " *Proc. IEEE Energy Convers. Congr. Expo*., Pittsburgh, PA, USA, pp. 1400-1407, Sep. 2014 .

[76] R. S. Rebeiro, and A. M. Knight, "Comparison of operating modes for a brushless doubly fed reluctance motor drive," *Proc. IEEE Energy Convers. Congr. Expo*., Cincinnati, OH, pp. 1323-1330, Oct. 2017.

[77] L. Ou, X. Wang, F. Xiong, and C.Ye, "Reduction of torque ripple in a wound-rotor brushless doubly-fed machine by using the tooth notching," *IET Eletr. Power Appl*., vol.12, no.5, pp. 635-642, 2018.

[78] P. Han, M. Cheng, X. Zhu, and Z. Chen, "Multifrequency spiral vector model for the brushless doubly-fed induction machine," *Proc. IEEE Electr. Mach. Drives Conf*., Miami, FL, USA, pp. 1-8, May 2017.

[79] E. Abdi, P. Malliband, and R. A. McMahon, "Study of iron saturation in brushless doubly-fed induction generators," *Proc. Energy Convers. Congr. Expo.*, Atlanta, GA, USA, pp. 3501-3508, Sep. 2010.

[80] H. Gorginpour, H. Oraee, E. Abdi, "Calculation of core and stray load losses in brushless doubly fed induction generators," *IEEE Trans. Ind. Electron.*, vol.61, no.7, pp. 3167-3177, 2014.

[81] F. Runcos, R. Carlson, N. Sadowski, P. Kuo-Peng, and H. Voltolini, "Performance and vibration analysis of a 75kW brushless doubly-fed induction generator prototype," *Proc. Ind. Appl. Soc. Annu. Meeting*, Tampa, USA, pp. 2395-2402, Oct. 2006.

[82] T. Logan, R. A. McMahon, and K. Seffen, "Noise and vibration in brushless doubly fed machine and brushless doubly fed reluctance machine," *IET Electr. Power Appl*., vol.8, no.2, pp. 50-59, 2014.

[83] C. D. Cook, and B. H. Smith, "Stability and stabilization of doubly-fed single-frame cascaded induction machines," *Proc. IEE*, vol.126, no.11, pp. 1168-1174, 1979.

[84] C. D. Cook, and B. H. Smith, "Effects of machine parameter values on dynamic response and stability regions of doubly-fed cascade induction machines," *Proc. IEE*, vol.130-part B, no.2, pp. 137-142, 1983.

[85] J. Poza, E. Oarbide, D. Roye, and I. Sarasola, "Stability analysis of a BDFM under open-loop voltage control," *Proc. Eur. Conf. Power Electr. Appl.*, Dresden, Germany, pp. P1-P10, Sep. 2005.

[86] Y. Tang, and L. Xu, "Stability analysis of a slip power recovery system under open loop and field oriented control," *Rec. Ind. Appl. Soc. Annu. Meeting*, Toronto, Canada, pp. 558-564, Oct. 1993.

[87] A. Kusko, and C. B. Somuah, "Speed control of a single-frame cascade induction motor with slip power pump back," *IEEE Trans. Ind. Appl.*, vol.IA-14, no.2, pp. 97-105, 1978.

[88] D. Zhou, R. Spée, and A. K.Wallace, "Laboratory control implementation for doubly fed machines," *Proc. Int. Conf. Ind. Electron. Contr. Instr.*, Maui, USA, pp. 1181-1186, Nov. 1993.

[89] M. G. Jovanović, R. E. Betz, and J. Yu, "The use of doubly-fed reluctance machines for large pumps and wind turbines," *IEEE Trans. Ind. Appl*., vol.38, no.6, pp. 1508-1516, 2002.

[90] I. Sarasola, J. Poza, E. Oyarbide, and M. A. Rodriguez, "Stability analysis of a brushless doubly-fed machine under closed loop scalar current control," *Proc. Ind. Electron. Conf.*, Paris, France, pp. 1527-1532, Nov. 2006.

[91] B. Hopfensperger, D. J. Atkinson, and R. A. Lakin, "Stator flux oriented control of a cascaded doubly-fed induction machine, " *IEE Proc.-Electr. Power Appl.*, vol.146, no.6, pp. 597-605, 1999.

[92] D. Basic, J. Zhu, and G. Boardman, "Transient performance study of a brushless doubly fed twin stator induction generator," *IEEE Trans. Energy Convers.*, vol.18, no.3, pp.400-408, 2003.

[93] K. Protsenko, and D. Xu, "Modeling and control of brushless doubly fed induction generators in wind energy applications," *IEEE Trans. Power Electron.*, vol.23, no.3, pp. 1191-1197, 2008.

[94] M. Cheng, R. Luo, and X. Wei, "Design and analysis of current control methods for brushless doubly-fed induction machines," *IEEE Trans. Ind. Electron*., DOI: 10.1109/TIE.2018.2829688.

[95] B. Hopfensperger, D. J. Atkinson, and R. A. Lakin, "Combined magnetizing flux oriented control of the cascaded doubly-fed induction machine," *IEE Proc.-Electr. Power Appl*., vol.148, no.4, pp. 354-362, 2001.

[96] G. Esfandiari, M. Ebrahimi, and A. Tabesh, "Instantaneous torque control method with rated torque sharing ratio for cascaded DFIMs," *IEEE Trans. Power Electron.*, vol.32, no.11, pp. 8671-8680, 2017.

[97] L. Xu, L. Zhen, and E. Kim, "Field orientation control of a doubly excited brushless reluctance machine," *IEEE Trans. Ind. Appl.*, vol.34, no.1, pp. 148-155, 1998.

[98] S. Ademi, and M. G. Jovanović, "Vector control methods for brushless doubly fed reluctance machines," *IEEE Trans. Ind. Electron*., vol.62, no.1, pp. 96-104, 2015.

[99] S. Ademi, M. G. Jovanović, and M. Hasan, "Control of brushless doubly-fed reluctance generators for wind energy conversion systems," *IEEE Trans. Energy Convers.*, vol.30, no.2, pp. 596-604, 2015.

[100] Y. Zhang, and J. G. Zhu, "Direct torque control of cascaded

brushless doubly fed induction generator for wind energy applications," *Proc. Int. Electr. Mach. Drives Conf*., Niagara, ON, Canada, pp. 741-746, May 2011.

[101] J. Hu, J. Zhu, and D. G. Dorrell, "A new control method of cascaded brushless doubly fed induction generators using direct power control," *IEEE Trans. Energy Convers*., vol.29, no.3, pp. 771-779, 2014.

[102] A. Broekhof, M. Tatlow, and R. McMahon, "Vector-controlled grid synchronization for the brushless doubly-fed induction generator," *Proc. IET Int. Conf. Power Electron. Mach. Drives*, Manchester, UK, pp. 1-5, Apr. 2014.

[103] R. Sadeghi, S. M. Madani, and M. Ataei, "A new smooth synchronization of brushless doubly-fed induction generator by applying a proposed machine model," *IEEE Trans. Sustain. Energy*, vol.9, no.1, pp. 371-380, 2018.

[104] W. R. Brassfield, R. Spée, and T. G. Habetler, "Direct torque control for brushless doubly-fed machines," *IEEE Trans. Ind. Appl*., vol.32, no.5, pp. 1098-1104, 1996.

[105] I. Sarasola, J. Poza, and M. A. Rodriguez, "Direct torque control design and experimental evaluation for the brushless doubly fed machine," *Energy Convers. and Manage*., vol.52, no.2, pp. 1226-1234, 2011.

[106] M. G. Jovanović, J. Yu, and E. Levi, "Encoderless direct torque controller for limited speed range applications of brushless doubly fed reluctance motors," *IEEE Trans. Ind. Appl*., vol.42, no.3, pp. 712-722, 2006.

[107] W. K. Song, and D. G. Dorrell, "Implementation of improved direct torque control method of brushless doubly-fed reluctance machines for wind turbine, " *Proc. IEEE Int. Conf. Ind. Tech*., Busan, Korea, pp.509-513, Feb./Mar. 2014.

[108] A. Zhang, X. Wang, W. Jia, and Y. Ma, "Indirect stator-quantities control for the brushless doubly fed induction machine," *IEEE Trans. Power Electron.*, vol.29, no.3, pp. 1392-1401, 2014.

[109] R. Zhao, A. Zhang, Y. Ma, X. Wang, and J. Yan, "The dynamic control of reactive power for the brushless doubly fed induction machine with indirect stator-quantities control scheme," *IEEE Trans. Power Electron.*, vol.30, no.9, pp. 5046-5057, 2015.

[110] G. Zhang, J. Yang, Y. Sun, M. Su, and W. Tang "A robust control scheme based on ISMC for the brushless doubly fed induction machine," *IEEE Trans. Power Electron.*, DOI: 10.1109/TPEL.2017.2708741, 2017.

[111] R. Sadeghi, S. M. Madani, M. Ataei, M. R. A. Kashkooli, and S. Ademi, "Super-twisting sliding mode direct power control of brushless doubly fed induction generator," *IEEE Trans. Ind. Electron*., DOI: 10.1109/TIE.2018.2818672, 2018.

[112] X. Wei, J. Zhu, M. Cheng, H. Yang, and B. Ma, "Model predictive control of brushless doubly fed twin stator induction machine: a model reduction approach," *Proc. Int. Conf. Electr. Mach. Syst*., Sydney, Australia, pp. 1-6, Aug. 2017.

[113] S. Shao, T. Long, E. Abdi, and R. A. McMahon, "Dynamic control of the brushless doubly fed induction generator under unbalanced operation," *IEEE Trans. Ind. Electron*., vol.60, no.6, pp. 2465-2476, 2013.

[114] J. Chen, W. Zhang, B. Chen, and Y. Ma, "Improved vector control of brushless doubly fed induction generator under unbalanced grid conditions for offshore wind power generations," *IEEE Trans. Energy Convers*., vol.31, no.1, pp. 293-302, 2016.

[115] I. A. Gowaid, A. S. Abdel-Khalik, A. M. Massoud, and S. Ahmed, "Ride-through capability of grid-connected brushless cascade DFIM wind turbines in faulty grid conditions - a comparative study," *IEEE Trans. Sustain. Energy*, vol.4, no.4, pp. 1002-1015, 2013.

[116] T. Long, S. Shao, P. Malliband, E. Abdi，and R. A. McMahon, "Crowbarless fault ride-through of the brushless doubly fed induction generator in a wind turbine under symmetrical voltage dips," *IEEE Trans. Ind. Electron*., vol.60, no.7, pp. 2833-2841, 2013.

[117] T. Long, S. Shao, E. Abdi, R. A. McMahon，and S. Liu, "Asymmetrical low-voltage ride through of brushless doubly fed induction generators for the wind power generation," *IEEE Trans. Energy Convers*., vol.28, no.3,pp.502-511, 2013.

[118] A. Oraee, E. Abdi, and R. A. McMahon, "Converter rating optimization for a brushless doubly-fed induction generator," *IET Renew. Power Gen.*, vol.9, no.4, pp. 360-367, 2015.

[119] M. Gholizadeh, A. Oraee, S. Tohidi, H. Oraee, and R. A. McMahon, "An analytical study for low voltage ride through of the brushless doubly-fed induction generator during asymmetrical voltage dips, " *Renew. Energy*, vol.115, pp. 64-75, 2018.

[120] S. Tohidi, H. Oraee, and M. R. Zolghadri, "Analysis and enhancement of low-voltage ride-through capability of brushless doubly fed induction generator," *IEEE Trans. Ind. Electron*., vol.60, no.3, pp.1146-1155, 2013.

[121] R. Gao, A. Zhang, S. Wang, and Z. Chen, "Improved crowbarless LVRT control strategy based on flux linkage tracking for brushless doubly fed induction generator," *Proc. IEEE Annu. Southern Power Electron. Conf*., Auckland, New Zealand, pp. 1-7, Dec. 2016.

[122] X. Chen, X. Wang, and F. Xiong, "Research on excitation control for stand-alone wound rotor brushless doubly-fed generator system," *Proc. Int. Conf. Electr. Mach. Syst*., Busan, South Korea, pp. 663-667, Oct. 2013.

[123] X. Chen, Z. Wei, and X. Gao, "Research of voltage amplitude fluctuation and compensation for wound rotor brushless doubly-fed machine," *IEEE Trans. Energy Convers*., vol.30, no.3, pp. 908-917, 2015.

[124] M. Lu, Y. Chen, L. Sun, X. Zou, and Y. Kang, "Control winding quantities orientation modeling and control for stand-alone brushless doubly-fed power generation system," *Proc. IEEE Energy Convers. Congr. Expo*., Montreal, Canada, pp. 2828-2833, Sep.2015.

[125] Y. Liu, W. Ai, and B. Chen, "Control design and experimental verification of the brushless doubly-fed machine for stand-alone power generation applications," *IET Electr. Power Appl*., vol.10, no.1, pp. 25-35, 2016.

[126] L. Sun, Y. Chen, J. Su. D. Zhang, and L. Peng, "Decoupling network design for inner current loops of stand-alone brushless doubly-fed induction generation power system, " *IEEE Trans. Power Electron*., vol.33, no.2, pp. 957-963, 2018.

[127] L. Sun, Y. Chen, L. Peng, and Y. Kang, "Numerical-based frequency domain controller design for stand-alone brushless doubly fed induction generator power system," *IET Power Electron*., vol.10, no.5, pp. 588-598, 2017.

[128] M. Cheng, Y. Jiang, P. Han, and Q. Wang, "Unbalanced and low-order harmonic voltage mitigation of stand-alone dual-stator brushless doubly fed induction wind generator," *IEEE Trans. Ind. Electron*., DOI: 10.1109/TIE.2017.2779422, 2017.

[129] X. Wang, H. Lin, and Z. Wang, "Transient control of the reactive current for the line-side converter of the brushless doubly-fed induction generator in stand-alone operation," *IEEE Trans. Power Electron.*, vol.32, no.10, pp. 8193-8203, 2017.

[130] X. Wang, and H. Lin, "DC-link current estimation for load-side converter of brushless doubly-fed generator in the current feed-forward control," *IET Electron.*, vol.9, no.8, pp. 1703-1710, 2016.

[131] L. Liao, and C. Sun, "A novel position sensorless control scheme for doubly fed reluctance motor drives," *IEEE Trans. Ind. Appl*., vol.30, no.5, pp. 1210-1218, 1994.

[132] H. Chaal, and M. G. Jovanović, "Practical implementation of sensorless torque and reactive power control of doubly-fed machines," *IEEE Trans. Ind. Electron.*, vol.59, no.6, pp. 2645-2653, 2012.

[133] M. G. Jovanović, and H. Chaal, "Wind power applications of doubly-fed reluctance generators with parameter-free hysteresis control," *Energy Convers. Manage*., vol.134, pp. 399-409, 2017.

[134] S. Ademi, M. G. Jovanović, and H. Chaal, "A new sensorless speed control scheme for doubly fed reluctance generators, " *IEEE Trans. Energy Convers.*, vol.31, no.3, pp. 993-1001, 2016.

[135] K. Kiran, and S. Das, "Sensorless speed estimation and control of brushless doubly-fed reluctance machine drive using model reference adaptive system," *Proc. IEEE Int. Conf. Power Electron. Drives Energy Syst.*, Trivandrum, India, pp. 1-6, Dec. 2016.

[136] K. Kiran, and S. Das, "Implementation of reactive power-based MRAS for sensorless speed control of brushless doubly fed reluctance motor drive," *IET Power Electron*., vol.11, no.1, pp.192-201, 2018.

[137] U. T. D. Shipurkar, and H. Polinder, "Achieving sensorless control for the brushless doubly-fed induction machine," *IEEE Trans. Energy Convers.*, vol.32, no.4, pp. 1611-1619, 2017.

[138] W. Tang, J. Yang, G. Zhang, Y. Sun, S. Ademi, F. Blaabjerg, and Q. Zhu "Sensorless control of brushless doubly-fed induction machine using a control winding current MRAS observer," *IEEE Trans. Ind. Electron*., DOI: 10.1109/TIE.2018.2831168, 2018.
[139] Y. Liu, F. Xiong, and F. Blaabjerg, "Sensorless direct voltage control of the stand-alone brushless doubly-fed generator," *Proc. Int. Conf. Electr. Mach. Syst*., Sydney, Australia, pp.1-6, Aug. 2017.
[140] Y. Liu, W. Xu, T. Long, and F. Blaabjerg, "A new rotor speed observer for stand-alone brushless doubly-fed induction generators," *Proc. IEEE Energy Convers. Congr. Expo*., Cincinnati, OH, USA, pp. 5086-5092, Oct. 2017.
[141] R. Carlson, H. Voltolini, F. Runcos, and P. Kuo-Peng, "Performance analysis with power factor compensation of a 75 kW brushless doubly fed induction generator prototype," *Proc. IEEE Int. Electr. Mach. Drives Conf*., Antalya, Turkey, pp. 1502-1507, May 2007.
[142] R. E. Betz, and M. G. Jovanović, "Theoretical analysis of control properties for the brushless doubly fed reluctance machine," *IEEE Trans. Energy Convers*., vol.17, no.3, pp. 332-339, 2002.
[143] R. E. Betz, and M. G. Jovanović, "The brushless doubly fed reluctance machine and the synchronous reluctance machine – a comparison," *IEEE Trans. Ind. Appl*., vol.36, no.4, pp. 1103-1110, 2000.
[144] A. M. Knight, R. E. Betz, and D. G. Dorrell, "Design and analysis of brushless doubly fed reluctance machines, " *IEEE Trans. Ind. Appl*., vol.49, no.1, pp. 50-58, 2013.
[145] L. Xu, B. Guan, and H. Liu, "Design and control of a high-efficiency doubly-fed brushless machine for wind power generator application," *IEEE Energy Convers. Congr. Expo*., Atlanta, GA, USA, pp. 2409-2416, Sep. 2012.
[146] M. Hsieh, Y. Chang, and D. G. Dorrell, "Design and analysis of brushless doubly fed reluctance machine for renewable energy applications," *IEEE Trans. Magn*., vol.52, no.7, pp.1-5, Article#: 8204705, 2016.
[147] T. Staudt, F. Wurtz, and L. Gerbaud, "An optimization oriented sizing model for brushless doubly fed reluctance machines: development and experimental validation, " *Electr. Power Syst. Res*., vol.132, pp.125-131, 2016.

Peng Han (S'12-M'17) received the B.Sc. and Ph.D. degrees in Electrical Engineering from the School of Electrical Engineering, Southeast University, Nanjing, China, in 2012 and 2017, respectively.

From November 2014 to November 2015, he was a joint Ph.D. student funded by China Scholarship Council with the Department of Energy Technology, Aalborg University, Aalborg, Denmark, where he focused on the brushless doubly-fed machines for wind energy conversion and high power drive. He is currently a Rsearch Scientist with the Center for High Performance Power Electronics (CHPPE), Department of Electrical and Computer Engineering, The Ohio State University. His current research interests include electric machines and power electronics.

Ming Cheng (M'01-SM'02-F'15) received the B.Sc. and M.Sc. degrees in Electrical Engineering from the Department of Electrical Engineering, Southeast University, Nanjing, China, in 1982 and 1987, respectively, and the Ph.D. degree from the Department of Electrical and Electronic Engineering, The University of Hong Kong, Hong Kong, in 2001.

Since 1987, he has been with Southeast University, where he is currently a Chair Professor in the School of Electrical Engineering and the Director of the Research Center for Wind Power Generation. From January to April 2011, he was a Visiting Professor with the Wisconsin Electric Machine and Power Electronics Consortium, University of Wisconsin, Madison. His teaching and research interests include electrical machines, motor drives for electric vehicles, and renewable energy generation. He has authored or coauthored over 380 technical papers and 4 books and is the holder of over 100 patents in these areas.

Prof. Cheng is a fellow of the Institution of Engineering and Technology. He has served as chair and organizing committee member for many international conferences. He is a Distinguished Lecturer of the IEEE Industry Applications Society(IAS) in 2015/2016.

Sul Ademi (M'12) received the B.Eng. and Ph.D. degrees in Electrical and Electronics Engineering from Northumbria University at Newcastle upon Tyne, U.K., in 2011 and 2014, respectively.

From 2015 to 2017, he was a Lead Researcher engaged in knowledge exchange and transfer partnership activities between University of Strathclyde, Glasgow, U.K and GE Grid Solutions, Stafford, U.K., where he focused on the development of novel DC protection schemes suitable for protecting future high-voltage direct current (HVDC) transmission systems. He is currently a Research Scientist with the Warwick Manufacturing Group, University of Warwick, Coventry, U.K. His main interests are in the areas of electric motor drives, validation of high-performance controllers for variable-speed applications, applications and control of doubly-fed machines, and design and analysis of novel permanent-magnet machines.

Milutin G. Jovanovic (M'99-SM'05) received the Dipl.Eng and M.E.E. degrees from the University of Belgrade, Belgrade, Serbia, in 1987 and 1991, respectively, and the Ph.D. degree from the University of Newcastle, Callaghan, Australia, in 1997, all in Electrical Power Engineering.

He is currently an Associate Professor with the Faculty of Engineering and Environment at Northumbria University, Newcastle upon Tyne, U.K. He has published more than 150 journal and conference papers including many book chapters. His major interests and activities are in the areas of reluctance machine drives, control and applications of doubly-fed motors and generators, and wind energy conversion systems.